UNESP - Universidade Estadual Paulista
Instituto de Química - Araraquara
Departamento de Química Analítica

TESE DE DOUTORADO

Magnetic Molecularly Imprinted Polymers (MMIPs) - synthesis and characterization for the spectrophotometric determination of caffeine

Shahab Ali

Araraquara
2019

Shahab Ali

Magnetic Molecularly Imprinted Polymers (MMIPs) - synthesis and characterization for the spectrophotometric determination of caffeine

Thesis submitted to the Instituto de Química da Universidade Estadual Paulista "Júlio de Mesquita Filho", as part of the requirements for obtaining the title of doctor in chemistry.

Orientadora: Prof.ª Dr.ª Maria Del Pilar Taboada Sotomayor

Araraquara

2019

FICHA CATALOGRÁFICA

Ali, Shahab
A398m Magnetic Molecularly Imprinted Polymers (MMIPS): synthesis and characterization for the spectrophotometric determination of caffeine / Shahab Ali. – Araraquara: [s.n.], 2019
95 p.: il.

Thesis (doctor) – Universidade Estadual Paulista, Instituto de Química
Advisor: Maria del Pilar Taboada Sotomayor

1. Imprinted polymers. 2. Nanoparticles. 3. Caffeine. 4. Magnetite. 5. Biomimetic materials. I. Title.

Elaboração: Seção Técnica de Aquisição e Tratamento da Informação Biblioteca do Instituto de Química, Unesp, câmpus de Araraquara

UNIVERSIDADE ESTADUAL PAULISTA

Câmpus de Araraquara

CERTIFICADO DE APROVAÇÃO

TÍTULO DA TESE: "Magnetic Molecularly Imprinted Polymers (MMIPs) - synthesis and characterization for the spectrophotometric determination of caffeine"

AUTOR: SHAHAB ALI

ORIENTADORA: MARIA DEL PILAR TABOADA SOTOMAYOR

Aprovado como parte das exigências para obtenção do Título de Doutor em QUÍMICA, pela Comissão Examinadora:

Profª. Drª. MARIA DEL PILAR TABOADA SOTOMAYOR
Departamento de Química Analítica / Instituto de Química - UNESP - Araraquara

Dr. ANTONIO APARECIDO PUPIM FERREIRA
Departamento de Química Analítica / Instituto de Química - UNESP - Araraquara

Prof. Dr. BRUNO CAMPOS JANEGITZ
Ciências da natureza, Matemática e Educação / Universidade Federal de São Carlos - UFSCAr - Araras

Videoconferência

Profª. Drª. REGINA MASSAKO TAKEUCHI
Faculdade de Ciências Integradas do Pontal / Universidade Federal de Uberlândia - UFU - Uberlândia

Profª. Drª. RENATA KELLY MENDES VALENTE
Faculdade de Química / Pontifícia Universidade Católica - PUC - Campinas

Araraquara, 22 de março de 2019

CURRICULUM VITAE

Personal information

Name: Shahab Ali

Date of Birth: 03 March, 1981

Nationality: Pakistani

Present address: Av: Luiz de Camões, 1118 casa 01 – Fundos, Bairro Quitandinha, Araraquara-SP

Email: shahab.chemist@gmail.com

Academic record

PhD (Analytical Chemistry). Instituto de Química –UNESP, Campus de Araraquara, Araraquara (SP), Brasil (2015 - 2019).

Master M.Sc. Analytical / Inorganic Chemistry. Hazara University Mansehra, Khyber Pukhtunkhwa (KPK), Pakistan, (2004 – 2006).

Graduation B.Sc. Botany / Zoology / Chemistry. Govt. Degree College Chota Lahor Sawabi, University of Peshawar, Khyber Pukhtunkhwa (KPK), Pakistan, 200.

.

Participation in events and conferences

1. ALI, S., AVILES-FELIX, L. KHAN, W.U., SOTOMAYOR, M.D.P.T. Magnetic Molecularly Imprinted Polymers (MMIPs) - synthesis and characterization for the

determination of caffeine. 18º Encontro Nacional de Química Analítica – ENQA. 18 a 21 de setembro de 2016, Florianópolis, Santa Catarina.

2. Participação em Workshop – ENQA 2016: Avanços em Química Analítica e Bioenergia – Homenagem Prof. Nelson R. Stradiotto.

3. Participação no Mini-curso – ENQA 2016: Assimilando a química forense: falta muito? Ministrado pelo Dr. Adriano O. Maldaner.

4. SIMPECTT.symposium

   September 13-14, 2018. Gray Amphitheater, block B6 superior, USP Sao Paulo.

Professional experience:

- ***Quality Control Manager*** (Feb 2010 – Feb 2015) **IPRAM International** Pharmaceuticals Islamabad.

Manufacturer of Liquid & Dry Injections, Dry suspension.

- ***Quality Control Manager*** (Oct 2009 – Feb 2010) **Grand Pharma (Pvt) Ltd. RCCI** Rawat Islamabad.

Manufacturer of Vet Oral Liquid, Dry Powder and Vaccines.

- ***Sr. Quality Control Analyst / QAI*** (Oct 2008 – Oct 2009) **VALOR Pharmaceutical**. Industrial Triangle Islamabad

Manufacturer of Tablet, Capsules, Cream, Ointments, Lotions and Sachets.

- ***Quality Control Analyst*** (April 2007 – Oct 2008) **Global Pharmaceutical** Industrial Triangle Islamabad.

Manufacturer of Tablet, Capsules, Cream, Oral Liquid & Dry Suspensions, Liquid & Dry Injections, and penicillin products

- ***Quality Control Analyst / QAI*** (Jun 2006 – Feb 2007) **VALOR Pharmaceutical**

  Industrial Triangle Islamabad

Manufacturer of Tablet, Capsules, Cream, Ointments, Lotions and Sachets

DEDICATION

To

My mother Zarbaha Begam and

My father Muhammad Anwar.

ACKNOWLEDEGEMENTS

First and foremost, I praise and thank Almighty Allah SWT, for his unlimited blessings in the form of strength and courage, to accomplish this work, and many great people, whose guidance and assistance make this task possible for me.

To my parents, for all affection, love and support and prayers to achieve my dreams and goals.

My beloved wife for his tremendous love and support making my life precious.

My brother and sisters for the affection, love and moments of joy, fun, laughter and shared sorrows.

To Profª Drª Maria Del Pilar Taboada Sotomayor for all the trust deposited, for the countless opportunities given, for all professional and personal teaching, for patience, encouragement and, especially, for her kindness to me.

To Professors Nelson R. Stradiotto, Maria Valnice Boldrin, Hideko Yamanaka and Fabíola Manhas Verbi Pereira for discussions, help and teaching. To all professors of my study and language courses.

To members and friends of GEAr for friendship, collaboration, discussions, and relaxation especially: Sabir, Marcos, Ademar, Rafael, Felipe, Juliano, Guilherme, Lucas Neres, Pedro, Gerson, Shakeel Zaib, Miguel, Mariana, Bruna and Bianca.

To Pakistani and Indian friends, especially Dr. Sajjad Hussain, Dr. Sajjad Ullah, Dr. Sardar Hussain, Mian Abdul Ali, Dr. Anees, Dr. Anwar Shamem, Dr. Ayaz Hassan, Dr. Sajjad Ali, Dr. Akbar Ali, Dr. Zia Ud Din, Majid Ali and Wasid Ullah for nice social activities, and Dr. Chanchal, Dr. Kishwar, Dr. Joy Roy and Denish Pardi for nice gathering and playing soccer.

To the great friends I made during these four wonderful years in Araraquara, for all conversations, laughter, jokes, distractions, companionship, tears, ballads and help in the difficult moments Andresa, Victor, Renan, Monica, Tarco, Douglas

To people who have welcomed me so well in Araraquara since 2015: Dona Vane, Odiny and Rafel family.

To all the employees and technicians of the Institute of Chemistry, which somehow contributed to the realization of this work,

To the Institute of Chemistry of UNESP for infrastructure and welcomed during these years.

Finally, to TWAS – CNPq fellowship for all financial support and opportunity for pos-graduation.

ABSTRACT

Daily food items contain considerable amount of caffeine that is constantly released to the environment, causing major problems to living organisms that can shift the entire ecosystem resulting adverse public health and the environment. Secondly, many market samples of caffeinated products have found with extremely high amounts of caffeine to toxic level (300 mg – 400 mg) that must be regulated by rapid techniques to assure human health and safety.

An alternative method for the detection and quantification is the development of biomimetic sensors, using magnetic molecularly imprinted polymers (MMIPs) like sensing phase. The advantages of molecular imprinted materials are high selectivity, sensitivity and stability, and low cost. This work aimed to develop an efficient method of preparation of core-shell magnetic nanoparticles (MNPs) modified with molecularly imprinted polymers (MIPs) used as selective material, in order to determine caffeine in the food samples in a very smart magnetic fashion. Metacrylic acid (MAA) was used as functional monomers; ethylene glycol dimethacrylate (EGDMA) was used as cross-linking reagents, *2,2'-azo-bis* isobutironitrila (AIBN) as a radical initiator and ethanol as pororgenic solvent. Magnetic molecularly non-imprinted polymers (MNIPs) which served as a control for comparative studies, synthesized along with MMIPs.

Characterizations of MMIPs and MNIPs were performed by Vibrating sample magnetometry (VSM), Fourier Transform Infra-Red (FTIR) and Transmission Electron Microscopy (TEM). The adsorption capacity and selectivity of the materials were studied in detail, from the respective adsorption isotherms and its kinetics. The adsorption data was well described by Langmuir-Freundlich isotherm model with adsorption equilibrium constant (K) of 9.6 x 10^2 mol L^{-1} which is higher in comparison with the reported. The selectivity experiments revealed that prepared MMIP had higher selectivity toward caffeine compared to other molecules with comparable chemical structures of theophylline and xanthine

Keywords: Magnetic nanoparticles (MNPs), molecularly imprinted polymers (MIPs), caffeine.

RESUMO

Muitos alimentos de uso diário contêm uma quantidade considerável de cafeína que é constantemente lançada ao meio ambiente, podendo causar grandes problemas aos organismos vivos que podem prejudicar todo o ecossistema, resultando em um problema de saúde pública e do meio ambiente. Adicionalmente, em muitas amostras de produtos cafeinados, comercializadas no mercado, tem apresentado quantidades extremamente altas de cafeína, chegando a níveis tóxicos (300 mg - 400 mg) e que devem ser monitoradas e reguladas por técnicas confiáveis e rápidas para garantir a saúde e a segurança dos consumidores.

Um método alternativo para a detecção e quantificação é o desenvolvimento de sensores biomiméticos, usando como fase seletiva de sensoriamento polímeros magnéticos molecularmente impressos (MMIPs). As vantagens dos materiais impressos moleculares são alta seletividade, estabilidade e baixo custo. Assim, este trabalho teve como objetivo desenvolver um método eficiente de preparação de nanopartículas magnéticas core-shell (MNPs) modificadas com polímeros molecularmente impressos (MIPs) utilizados como material seletivo, a fim de determinar a cafeína nas amostras de alimentos. O ácido metacrílico (MAA) foi usado como monômero funcional; metacrilato de etilenoglicol (EGDMA) como reagente de reticulao, 2,2'-azo-bis-isobutironitrila (AIBN) como iniciador radicalar e etanol como solvente porogênico. Polímeros magnéticos não impressos (MNIPs) que serviram como controle para estudos comparativos, foram também sintetizados junto com MMIPs.

As caracterizações dos MMIPs e MNIPs foram realizadas por magnetometria da amostra vibrante (VSM), infravermelho por transformada de Fourier (FTIR) e microscopia eletrônica de transmissão (TEM). A capacidade de adsorção e seletividade dos materiais foram estudadas em detalhe, a partir das respectivas isotermas de adsorção e de sua cinética. Os dados de adsorção foram bem descritos pelo modelo isotérmico de Langmuir-Freundlich com constante de equilíbrio de adsorção (K) de 9,6 x 10^2 mol L^{-1}, que é maior em comparação com o relatado. Os experimentos de seletividade revelaram que o MMIP preparado apresentou maior seletividade em relação à cafeína em comparação com outras moléculas com estruturas químicas análogas de teofilina e xantina.

Palavras-chave: Nanopartículas magnéticas (MNPs), molecularmente imprimidos polímeros (MIPs), cafeína.

Figures List

Figure 1-1 The caffeine content of some of our favorite drinks 18
Figure 1-2 Caffeine effects on spider 20
Figure 1-3 Caffeine Molecule structure. 21
Figure 1-4: Caffeine and Adenosine Molecular Structures 22
Figure 1-5: Caffeine and its immediate metabolites; CYP refers to the enzymes catalyzing the reactions.[26] 23
Figure 1-6 Basic theme of MIP's synthesis. Step 1: interaction of Template with Functional Monomer in porogenic solvent, Step 2: formation of Template-Monomer Complex (TMC), Step 3: Polymerization of Cross-linker around TMC, Step 4: Template removal leaving imprinted cavities. 26
Figure 1-7 MIP synthesis illustration 27
Figure 3-1: The simulations evaluate the energy of the interaction caffeine with the 20 monomers proposed in Table 4. 42
Figure 3-2. Synthesis and modification of magnetite nanoparticles I, II, III. 44
Figure 3-3: Schematic representation for the synthesis of MIP for caffeine. 45
Figure 3-4: Photography of the system used in synthesis of MMIP for Caffeine and the respective MNIP. 46
Figure 3-5: Photography of the Soxhlet system used for cleaning of MIPs and NIPs (Left: Solvent heating evaporation. Middle: washing polymer. Right: Vapor condensation. 48
Figure 3-6: Photography of the homogenizer used in MIP/template reconnection assays. 49
Figure 4-1: The simulation evaluates the energy of the interaction caffeine with the 20 monomers proposed. 53
Figure 4-2: FTIR spectrum of methacrylic acid (MAA), Caffeine, EGDMA, TEOS, and AIBN. 56
Figure 4-3: Spectrum in the IR region for different stages of synthesis (Fe_3O_4, Fe_3O_4@SiO_2, Fe_3O_4@SiO_2-MPS, MNIP and MMIP). 57
Figure 4-4 ;TEM images of magnetite Fe_3O_4 (a) 200 nm, (b) 100 nm, and (c) 50 nm magnification and (d) size distribution histogram of magnetite. 58

Figure 4-5: TEM images of (a) 1 µm, (b) 500 nm, (c) 200 nm, (d) 100 nm, and (e) 50 nm magnification of Fe_3O_4@SiO_2 and (f) size distribution histogram. 60
Figure 4-6: TEM images of (a) 500 nm, (b) 100 nm, and (c) 50 nm magnification of Fe_3O_4@SiO_2-MPS and (d) size distribution histogram.....62
Figure 4-7: TEM images of 1 µm magnification of (a) MNIP, and (b) of MMIP.....63
Figure 4-8: Illustration of the magnetic moment (M) of different types of materials under application a magnetic field (H).....65
Figure 4-9: The magnetization curves of Fe_3O_4, Fe_3O_4@SiO_2, Fe_3O_4@SiO_2-MPS obtained in this work.....66
Figure 4-10: The magnetization curves of Fe_3O_4@MIP of polymers. 67
Figure 4-11: The magnetization curves of Fe_3O_4@NIP of polymers.. 67
Figure 4-12: Absorption spectrum in the UV-Vis region for different concentrations of Theophylline and Xanthene soluble in water and dilute NaOH (aqueous) respectively.....68
Figure 4-13: Analytical curve referring to the maximum absorbance at wavelength 278 nm, used like solvent methanol. 69
Figure 4-14: Calibration curve for caffeine - CAF (a), theophylline - TEPH (b) prepared in deionized water and (c) xanthine - XAN in 0.01 mol L^{-1} NaOH solution. 71
Figure 4-15: Chromatograms obtained for Caffeine, under 3.3. procedure. 72
Figure 4-16: Analytical curve for caffeine obtained in HPLC/UV-Vis, in conditions previously described in 3.3. section. 73
Figure 4-17: Purification Washing procedure. I) Magnetic separation, II) Bulk Washing, III) Soxhlet extractor. 75
Figure 4-18: Results for optimizing the interaction time (analyzed range 10 to 120 Minutes) between MMIP (10 mg mL^{-1}), caffeine (20.0 mg L^{-1}) prepared in methanol. 76
Figure 4-19: Results for optimizing the interaction time (analyzed range 20 to 240 minutes) for 1 mgL^{-1} polymer of 20.0 mg L^{-1} caffeine prepared in water. 77
Figure 4-20: 20 mg L^{-1} Caffeine adsorption profile as function of pH in the range from 3.0 to 11.0 to 0.5 mg mL^{-1} MMIP and MNIP at interaction time to 40 min. 78
Figure 4-21: Caffeine adsorption isotherm (in the concentration range of 20 to 480 mg L^{-1}) to MMIP (or MNIP) at 1.0 mg mL^{-1} of polymer to interact for 40 min and pH 7.0. 79
Figure 4-22: Adsorption isotherm for comparison of selectivity (THP-Theophylline).....80
Figure 4-23: Adsorption isotherm for comparison of selectivity (XTN-Xanthine).....80

Figure 4-24: Adsorption isotherms for comparison of selectivity (CAF-Caffeine, THP-Theophylline, and XTN-Xanthine until 320 mg L-1 for 1.0 mg mL-1 of materials).81
Figure 4-25: Real sample treatment analysis. 84
Figure 4-26: Chromatograms obtained in the analysis of samples. 84

List of Tables

Table 1: Functional Monomers classified on types of bonding generally carried out[58] 29
Table 2: Common Cross-linkers classified on types of bonding generally carried out [59] 30
Table 3: Common polymerization initiators used in the synthesis of MIPs[59] 32
Table 4: Monomers commonly used in the synthesis of MIP and chosen to perform the computational simulation[60]. 41
Table 5: Reagent amounts used for the different MMIPs and MNIPs synthesized in this work.47
Table 6: Dilution chart of beverage samples. Samples diluted nearly to 40 ppm caffeine concentration. Polymer mass 2mg; spread over 120 min in 1.0 mL of an aqueous solution. 52
Table 7: Size distribution of Magnetic Nanoparticles 63
Table 8: Binding parameters for MMIP and MNIP for Caffeine in comparison with theophylline and xanthine. 82
Table 9: Recovery values obtained in the beverage food analysis compared with the Blank values.....85
Table 10: Concentration in ppm of the caffeine in the solution after adsorption experiments and the samples, which were evaluated and estimated by HPLC method. 85

LIST OF ABBREVIATIONS AND ACRONYMS

1VI: 1-vinylimidazole

ABDV: 2,2'-azo- *bis*- (2,4-dimethylvaleronitrile)

Abs: Absorbance

ACN: Acrylonitrile

AIBN: 2,2'-azo- *bis*- (2-methylpropionitrile)

AMPSA: 2-Acrylamido-2-methylpropane sulfonic acid

APM: 4,4'-diaminodiphenylmethane

BET: Brunauer, Emmett, Teller (Multimolecular Adsorption Theory)

BR: Britton-Robinson

HPLC: High Performance Liquid Chromatography

DNA: deoxyribonucleic acid

EGDMA: Ethylene Glycol Dimethacrylate

FEG-SEM: High-resolution scanning electron microscopy with field emission electron source

FTIR: Infrared with Fourier transform

IUPAC - International Union of Pure and Applied Chemistry

MAA: Methacrylic acid

MMIP: Magnetic Molecularly Imprinted Polymer

MNIP: Magnetic Nonprinted Polymer

SM: Structural monomer

FM: Functional monomer

MeOH: Methanol

MF: Functional monomer

MIP: Molecularly imprinted polymer

MPS: 3-methacryloxy-propyl-trimethoxysilane

NIP: Nonimprinted Polymer

SPE: Solid phase extraction

UV-Vis: Ultraviolet-Visible

TABLE OF CONTENTS

1 Introduction 18

1.1 Caffeine Determination 25

1.2 Molecularly printed polymers (MIPs) 25

1.3 Core-shell Magnetic Molecularly Imprinted Polymer 33

1.4 Kinetic studies in MIPs 34

1.4.1 Adsorption isotherms obtained for template affinity studies with MIP 34

1.5 Application of Molecularly Imprinted Polymers (MIP) 36

2 Objective 38

3 Material and Methods 39

3.1 REAGENTS AND SOLUTIONS 39

3.2 INSTRUMENTATION 39

3.3 CHROMATOGRAPHIC METHOD 40

3.4 COMPUTATIONAL SIMULATION 41

3.5 EXPERIMENTAL PROCEDURES 43

3.5.1 Synthesis of magnetite nanoparticles 43

3.5.2 Synthesis of magnetic MIP 44

3.5.3 Study of adsorption kinetics of molecularly imprinted polymers 48

3.5.4 Adsorption isotherms 49

3.5.5 Optimization of Spectroscopic conditions for Caffeine analysis 49

3.5.6 Studies of optimization and evaluation of the efficiency of polymers 50

3.5.7 Evaluation of solvent, mass dosage and time 50

3.5.8 Rebinding and selectivity 51

3.5.9 Application of MMIP in food samples 51

4 Results and Discussion 53

4.1 COMPUTATIONAL SIMULATION 53

4.2 CHARACTERIZATION 54

4.2.1 Fourier transform infrared spectroscopy (FTIR) 54

4.2.2 Morphological characteristics 57

4.2.3 Vibrating sample magnetometry (VSM) 64

4.2.4 UV-vis behavior 68

4.3 CHROMATOGRAPHIC METHOD 71

4.4 REMOVAL OF THE CAFFEINE MOLECULE FROM THE MIP STRUCTURE 73

4.5 MMIP OPTIMIZATION EXPERIMENTS 75

4.6 ADSORPTION ISOTHERM, SELECTIVITY AND AFFINITY CONSTANTS (K_A) ... 78

4.7 Application in beverage samples 83

5 Conclusions - Perspectives 87

6 References 89

1 Introduction

Caffeine in the world's most widely consumed psychoactive drug classified as central nervous system(CNS) methyl xanthine class of stimulant.[1] It reversibly blocks the action of adenosine on its receptor and consequently prevents the onset of drowsiness induced by adenosine. Caffeine also stimulates certain portions of the autonomic nervous system[2].

Found commonly in the seeds, nuts, or leaves of a number of plants native to South America and East Asia. A well-known source of caffeine is the coffee bean, a misnomer for the seed of *Coffea* plants. Caffeine is extracted by steeping the plant product in water, a process called infusion. Caffeine-containing drinks, such as coffee, tea, and cola, are very popular (Figure 1.1). As source of 2014, 85% of American adults consumed some form of caffeine daily, consuming 164 mg on average.[3]

Figure 1-1 The caffeine content of some of our favorite drinks
Source: http://elaineallertondietitian.com/blog/caffeine. Accessed in March, 9th 2019.

History of coffee dates back to the 10th century, its origin thought to have been Ethiopia. The earliest substantiated evidence of either coffee drinking or knowledge of the coffee tree is from the 15th century, in the Sufi monasteries of Yemen.[4] By the 16th century, it had reached the rest of the Middle East, South India, Persia, Turkey, Africa. Coffee then spread to the Balkans, Italy and to the rest of Europe, to South East Asia and then to America.[5]

Caffeine is classified by the US Food and Drug Administration as "generally recognized as safe" (GRAS). Toxic doses, over 10 grams per day for an adult, are much higher than typical doses of under 500 milligrams per day. A cup of coffee contains 80–175 mg of caffeine, depending on what "bean" (seed) is used and how it is prepared (e.g. drip, percolation, or expresso). Thus, it requires roughly 50–100 ordinary cups of coffee to reach a lethal dose. However, pure powdered caffeine, which is available as a dietary supplement, can be lethal in tablespoon-sized amounts.

After water, coffee, tea, and soft drinks containing high amounts of caffeine are the most consumed beverages in our daily life. According to the study by US-FDA, the daily average American consumption of 300 mg caffeine[6], and metabolize about 95-98% into paraxanthine, theobromine, and theophylline. In highly populated areas, the excreted caffeine then goes through standardized wastewater treatment where, on average, 60-70% of the remaining caffeine, and is removed, and the rest enters the local streams and rivers intact.

In its natural plant caffeine functions as a pesticide, inhibits enzymes in insects' nervous systems, enduring reproductive harm, triggering paralysis and death in the more susceptible bugs[7]. Before dying, the adult and larval insects show, unnatural behaviors; for example, the larvae of mosquitoes may lose the ability to swim up to the water's surface and drown. Spiders fed caffeine-laced flies showed disorientation, incapable of creating symmetrical webs[8] (Figure 1.2).

Figure 1-2 Caffeine effects on spider

Source: https://owlcation.com/stem/Caffeine-Its-effects-on-animals-plants-and-the-environment. Accessed in March, 9th 2019.

Caffeine is more lethal when roughage and snails exposed to 0.5% caffeine solutions die within days, by increasing heart rate faster at concentrations of 0.1% and above, caffeine triggered deadly erratic and slowed pulse [9].

Larger forms of life succumb to the power of caffeine as well. By spraying caffeinated water on coqui frogs, the Hawaiian Department of Agriculture planned to perform mass amphibicide on the nuisance species with drug-induced heart attacks, forever silencing the amphibians' loud, shriek-like calls [10]. Luckily for the frogs, a lack of public support prevented the plan's actual implementation.

A wild parrot 20 gram caffeine in dark chocolate caused, irreparable damage of its liver, kidneys, and brain neurons[11]. A caffeine pill in German Shepherd displayed symptoms of overheating, an elevated heart rate, and agitated behavior before dying (for dogs the lethal dose is 140 mg per kilogram body weight)[12].

A major concern to environmentalists, for mollusks, tadpoles, snails, and other aquatic life. Caffeine molecule is significantly more toxic than it is to humans, harmful even at 0.097 mg L^{-1}.[2.] A recent study on inter-tidal salt-water mollusks, discovered that they produce significant

amounts of stress proteins when exposed to concentrations as low as 50 ng L^{-1}, and while caffeine does not bio-accumulate, reduced populations of these organisms could cause major shifts in the entire ecosystem.

Caffeine 1,3,7-trimethylxanthine (Figure 1.3), have the formula $C_8H_{10}N_4O_2$, molecular weight of 194.19 g mol^{-1}, a bitter taste, white color and melting point between 235–238 °C. It is moderately soluble in water; 2 g for each 100 mL, while very soluble in boiling water; 66 g for each 100 mL.[13.] Moderately soluble in ethanol 1.5 g/100 mL, weakly basic; pK_a of conjugate base of ~0.6, requiring strong acid to protonate it.[14] Caffeine not containing stereogenic centers[15] and hence is achiral. Its xanthine core contains two fused rings, a pyrimidinedione and imidazole. The pyrimidinedione contains two amide functional groups; all six of the atoms within the pyrimidinedione ring system are sp^2 hybridized and planar. Hence the fused 5,6 ring core of caffeine contains a total of ten pi electrons and according to Hückel's rule is aromatic.[16]

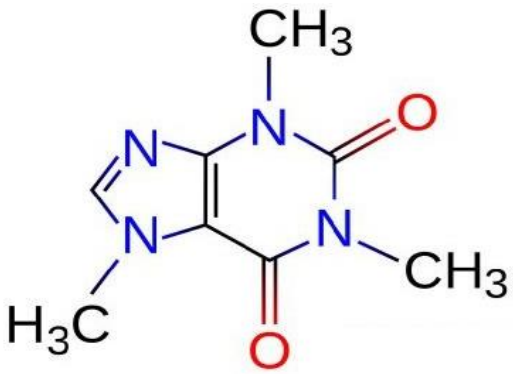

Figure 1-3 Caffeine Molecule structure.

Source: Own authorship

Caffeine mechanism of action principally is antagonist of adenosine[17]. In normal conditions when a person is alert in the absence of caffeine, little adenosine is present in the neurons of the CNS (Central Nervous System). Continued alertness over time accumulates adenosine in the neuronal synapse, binding and activating adenosine receptors on CNS neurons; causing the production of a cellular response that ultimately increases drowsiness. Caffeine antagonizes adenosine receptors; prevents adenosine from activating the receptor by blocking the

adenosine binding. This results, in a temporarily prevent or relieves drowsiness, and thus maintains or restores alertness[18].

Caffeine is both water- and lipid-soluble, and for this reason it readily crosses the blood–brain barrier. The caffeine molecule is structurally similar to adenosine (Figure 1-4), and is capable of binding to adenosine receptors on the surface of cells without activating them, thereby acting as a competitive antagonist[19].

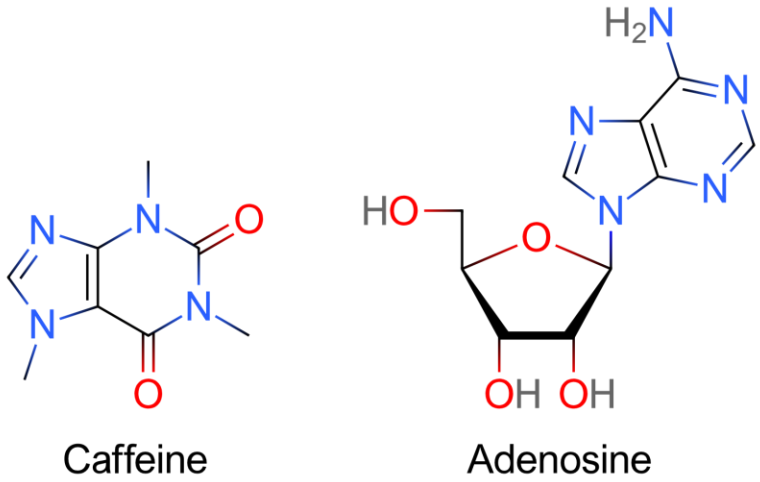

Figure 1-4: Caffeine and Adenosine Molecular Structures
Source: Own authorship

Caffeine antagonizes adenosine A2A receptors in the ventrolateral preoptic area (VLPO), thereby reducing inhibitory GABA neurotransmission to the tuberomammillary nucleus, a histaminergic projection nucleus that activation-dependently promotes arousal[20]. Disinhibition of the tuberomammillary nucleus is the chief mechanism by which caffeine produces wakefulness-promoting effects[21].

Caffeine from food is absorbed by the small intestine within 45 minutes of ingestion[22]. Peak blood concentration is reached within one hour and it is eliminated by first-order kinetics[23], [24]. Caffeine is metabolized in the liver by the *cytochrome P450 oxidase enzyme system* [25], in particular, by the CYP1A2 isozyme, into three primary metabolites:

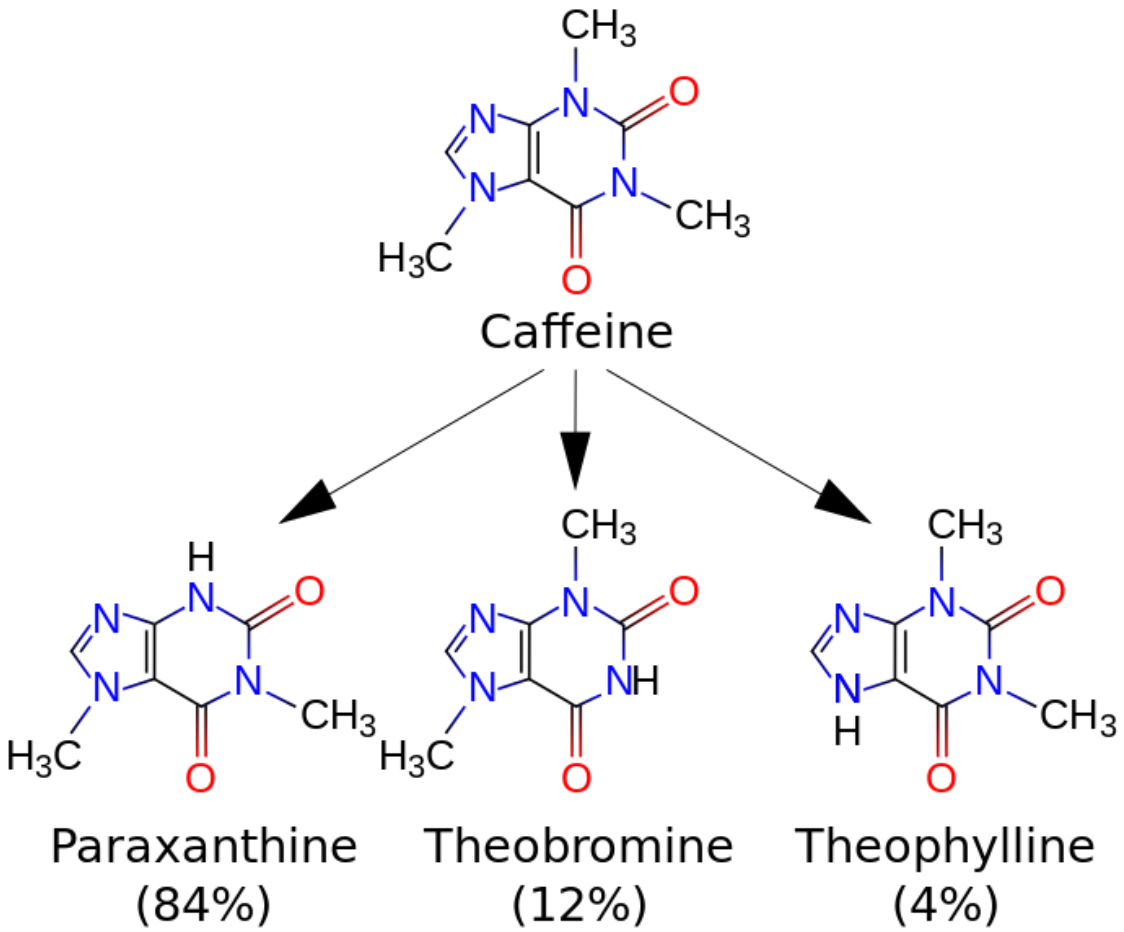

Figure 1-5: Caffeine and its immediate metabolites; CYP refers to the enzymes catalyzing the reactions.[26]

In which:

Paraxanthine: increases lipolysis, leading to elevated glycerol and free fatty acid levels in the blood plasma.

Theobromine: dilates blood vessels and increases urine volume. Theobromine is also the principal alkaloid in the cocoa bean, and therefore chocolate.

Theophylline: Relaxes smooth muscles of the bronchi, and is used to treat asthma. These metabolites then further metabolized and then excreted in the urine[27].

Caffeine had some major health benefits and also some adverse effects on human body. High long-term caffeine consumption is associated with a lower risk of cardiovascular disease and diabetes and also reducing risk of Alzheimer's disease. Low doses of caffeine show

increased alertness and decreased fatigue. Caffeine has been shown to increase the metabolic rate. Caffeine is studied as a treatment for the Parkinson's disease motor symptoms. Caffeine may lower the risk of developing type 2 diabetes[28,29].

Caffeine can increase blood pressure in non-habitual consumers. High blood pressure is associated with an increase in strokes, and cerebral vascular disease, which in turn increase the risk of multi-infarct dementia. Caffeine may reduce control of fine motor movements (e.g. producing shaky hands). Caffeine can contribute to increased insomnia and sleep latency. Caffeine withdrawal can produce headache, fatigue and decreased alertness. High doses of caffeine (300 mg or higher) can cause anxiety[30].

Caffeine overdose can result in a state of central nervous system over-stimulation called caffeine intoxication (DSM-IV 305.90)[31]. This syndrome typically occurs only after ingestion of large amounts of caffeine, more than 400–500 mg at a time[32]. The symptoms of caffeine intoxication are comparable to the symptoms of overdoses of other stimulants: they may include restlessness, anxiety, excitement, insomnia, flushing of the face, increased urination, gastrointestinal disturbance, muscle twitching, a rambling flow of thought and speech, irritability, irregular or rapid heartbeat, and psychomotor agitation.

In cases of much larger overdoses, mania, depression, lapses in judgment, disorientation, disinhibition, delusions, hallucinations, or psychosis may occur, and rhabdomyolysis (breakdown of skeletal muscle tissue) can be provoked[33]. But, in extreme overdose can result in death.[34]

The median lethal dose (LD50) given orally in humans is dependent on individual sensitivity, but is estimated to be about 150 to 200 milligrams per kilogram of body mass (80 to 100 cups of coffee for an average adult)[35].

It is easier to reach high doses with caffeine pills, and the lethal dose can be lower in individuals whose ability to metabolize caffeine is impaired. Chronic liver disease is one factor that can slow the metabolism of caffeine[36].

To evaluate and monitor environmental impacts of caffeine together with qualitative and quantitative determination in food samples, it is important to develop materials and methods[37], that allow the selective detection of these molecules, as well as their quantification with high sensitivity with low cost speedy on spot analysis. For achieving these high characteristics, recently employed advance sensitive materials known as molecularly imprinted polymers (MIP) that mimicking the biological interaction of antigen antibody or enzyme substrate like

interactions[38], and can achieve the desired analytical results with a superiorly high selective and sensitive fashion[39].

1.1 Caffeine Determination

Caffeine determination in foods using various quantitative techniques, such as: UV-spectrophotometry[40], High-Performance Liquid Chromatography coupled to Mass Spectrometry (HPLC-MS)[41,42] and capillary electrophoresis.[37] Recently electrochemical methods have been proposed[43], for example Sharma et al. prepared an electrochemically polymerized sensor that gave results with low sensitivity, showed high selectivity due to the stability of electrochemically obtained molecular imprinting polymer (MIP).[44]

The innovative synthesis of molecularly imprinted polymers (MIPs) has proven to be a distinct method for selective determination and quantification of several molecules. These are polymers with high selective recognition sites in the form of cavities, that are complementary to the analytes structure functionality;[45] mimicking the affinity-based biological recognition system also being referred as biomimetic polymers, similar to the specific enzyme-substrate or antigen-antibody systems.

1.2 Molecularly printed polymers (MIPs)

The rationale uses of template (target molecule) to selectively bind to a specific recognition site was suggested by Mudd in 1932 and then Pauling in 1940[46]. In 1942, Linus Pauling described the preparation of artificial antibodies using antigen molecules as template. In 1949 through Frank Dickey carried out the first work using printed synthetic product (silica gel) in the selective adsorption of methyl orange.[47]The development of molecular imprinted synthetic polymers, better known as MIP (Molecularly Imprinted Polymers) has been used to obtain systems with biomimetic recognition capabilities similar to the specific enzyme-substrate and/or antigen-antibody systems,[48] as illustrated in Figure 1.6 below.

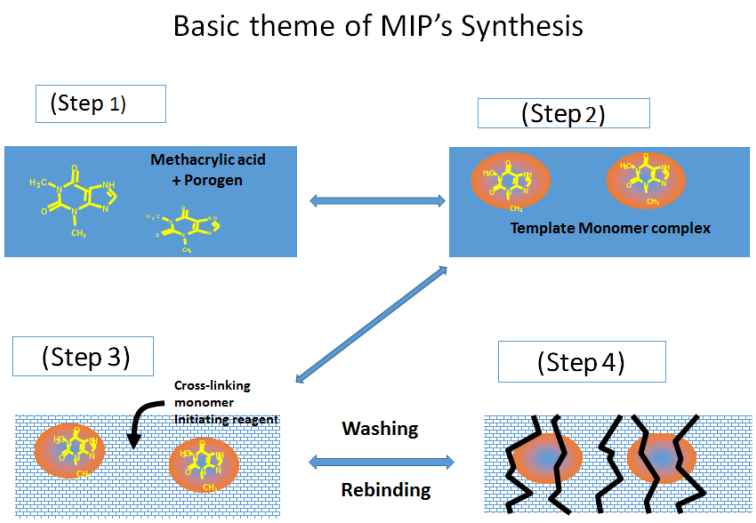

Figure 1-6 Basic theme of MIP's synthesis. Step 1: interaction of Template with Functional Monomer in pororgenic solvent, Step 2: formation of Template-Monomer Complex (TMC), Step 3: Polymerization of Cross-linker around TMC, Step 4: Template removal leaving imprinted cavities.
Source: Own authorship

Among the advantages offered by MIP can be mentioned: low cost; possibility of synthesis in situations where no biomolecule (receptor or enzyme) exists; resistance to adverse environments in which natural biomolecules would not withstand as in the presence of acids, bases, organic solvents and high temperatures.[49]

Molecular imprinted polymers (MIP) have been reported to exhibits significantly high affinity for the molecules used as the template than for similar molecules including closely related isomers. In recent years, MIPs have attracted much attention due to their outstanding advantages, such as predetermined recognition ability, stability, relative ease and low cost of preparation, and potential application to a wide range of target molecules. MIPs can, not only concentrate but also selectively separate the target analytes from complex samples.[50,51]

MIP synthesis involves, analyte molecule used as a template interacts by covalent or non-covalent bonds with the molecules of one or more type of functional monomers, forming first the Template-Monomer Complex (TMC). Subsequently polymerizing agent is added to the medium that promotes crosslinking and form a rigid polymer matrix around TMC. The polymerization reaction starts by employing heat, light, and the addition of a radical initiator. After completing polymerization, template molecules then removed from the polymer matrix, leaving behind

complementary cavities also known as recognition sites, by washing with solvent or by means of chemical cleavage if the molecule establishes covalent attachment with the monomer. The resulting polymer having uniform sized cavities capable of selectively holding the template molecule present in a complex sample. Non-imprinted Polymers (NIP) synthesized simultaneously sidewise utilizing exact materials and methods except not using the template (analytes free) as a standard for comparative analysis of MIP to serve as a control polymer.[52] MIPs emphasizing its worth employed as biomimetic compared to usual analysis techniques. Below is an illustrative schematic of MIP synthesis and the removal of the template molecule as shown in Figure 1.7 bellow.

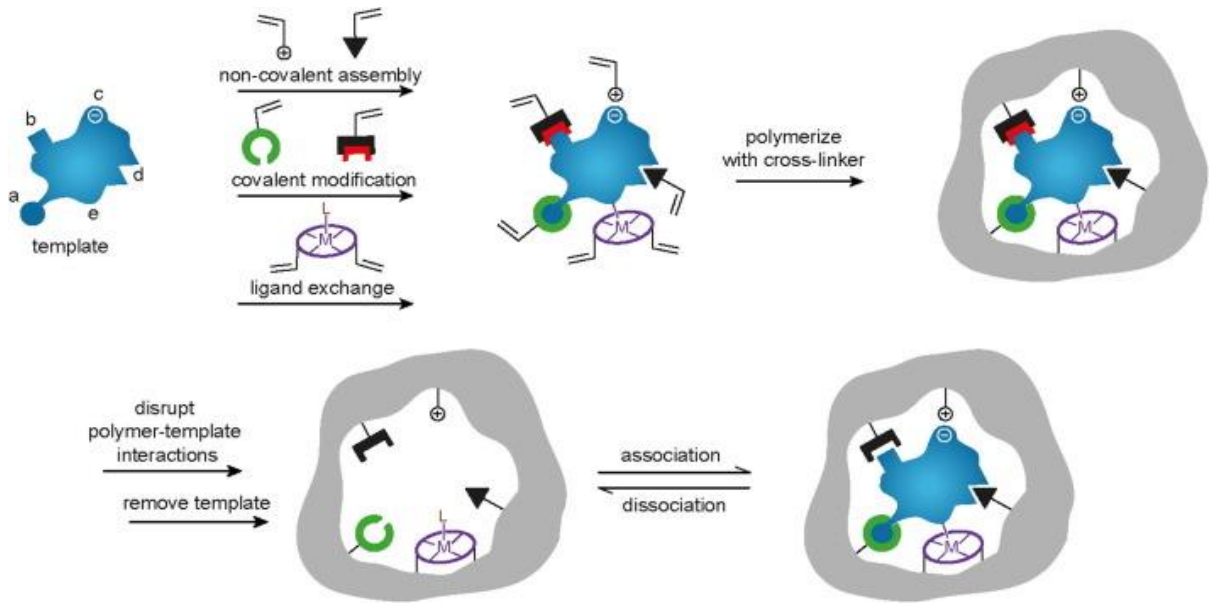

Figure 1-7 MIP synthesis illustration.

Source: H.F. EL-Sharif ET AL, 2015[53]

Schematic representation of the imprinting process, synthetic strategy involves one or more of the following interactions: (a) reversible covalent bonds, (b) covalently attached polymerizable binding groups that are activated for non-covalent interaction by template cleavage (sacrificial spacer or semi-covalent strategy), (c) electrostatic interactions, (d) hydrophobic or van der Waals interactions, (e) co-ordination with a metal center. Each, (a–e)

respectively are formed with complementary functional groups or structural elements of the template. Subsequent polymerization in the presence of a cross-linker produces a porous matrix in which template sites are located. For MIP synthesis, it is important to evaluate the choice of the reagents. The template molecule is responsible for the definition of the spatial organization of the functional groups with the functional monomers.[54]

The functional monomer is responsible for the interactions that will form between the polymer and analyte in the specific cavity formed.[55] The main purpose of the structural monomer is to stabilize the binding sites with molecular recognition and mechanical stabilization of the polymer matrix[56], and the type and amount of these reagents has great impact on the physical and chemical characteristics of the MIP.[57] Hence the cavities formed are contrary identical to the functional groups of molecular structure of that template, which is the main bases for templet selective recognition, and resulted MIP are stable structures which can be stored for long time and can be utilized in various different environments.

The radical initiator will initiate the free radical polymerization reaction basically in two ways: thermal or UV radiation.[31] The porogenic solvent of the medium should not interfere with the analyte-monomer interaction and is also responsible for the formation of pores in the polymer.[54]

The idea of covalent bonding involving template and functional monomer was introduced by Wulff and Sarchan.[32] In this work the template is removed from the polymer by cleavage of the covalent bonds. The high stability of the bonds formed between template and monomers leads to the formation of a large number of homogeneous binding sites, minimizing the existence of nonspecific binding sites. It should be noted that when the template is covalently attached to the functional monomer, in its subsequent application, the interactions are expected to be of the non-covalent type.

The concept of non-covalent interaction was introduced by Arshady and Mosbach.[33] Non-covalent interactions occur between specific functional groups on the polymerizable monomers and the template in the pre-polymerization mixture. These interactions can be of the type hydrogen bonds, ionic, hydrophobic interactions, among others. The non-

covalent procedure is considered the most widely used molecular imprinting method and has been applied to a wide variety of molecules. This is due to the fact that this type of interaction presents high versatility and applicability.

Among the various monomers and crosslinking agents reported in the literature, few were used in most studies. Usually the most commonly used functional monomers given in Table 1 include methacrylic acid, 2- and 4-vinylpyridines, trifluoromethylacrylic acid, acrylamide and hydroxyethylmethacrylate.

Table 1: Functional Monomers classified on types of bonding generally carried out[58]

Common Types	Functional monomers	Molecular Structure
(A) Covalent	**(1)** 4-Vinyl benzene boric acid; (**2**) 4-vinyl benzaldehyde; (**3**) 4-vinyl aniline; (**4**) *tert*-butyl *p*-vinylphenylcarbonate.	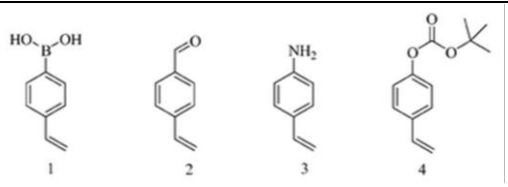
(B) Non-covalent	(**5**) acrylic acid (AA); (**6**) methacrylic acid (MAA); (**7**) trifluoromethyl acrylic acid (TFMAA); (**8**) methyl methacrylate (MMA);	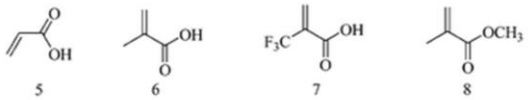
(C) Semi-covalent	(**9**) 3-Isocyanatopropyltriethoxysilane (IPTS)	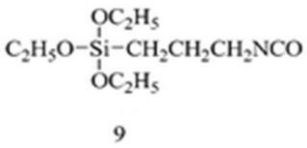
(D) Ligand exchange	(**10**) Cu (II)-iminodiacetate-derivatized vinyl monomer; (**11**) Fe^{2+}/MAA complex	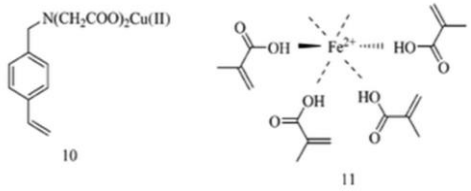

Crosslinking agents (Table 2) include glycol dimethacrylate (EGDMA), divinylbenzene and trimethylolpropyl trimethylacrylate (TRIM).

On the other hand, it should also be visualized that the efficiency in the formation of the binding sites in the MIP, is highly influenced by the chemical nature of the template. For this, the template must be stable and inert during polymerization and have functional groups that can interact with the functional groups of the monomer(s). The functional monomer plays an important role in the synthesis of MIP, since it is closely related to the formation of the binding sites with the template molecule.

Table 2: Common Cross-linkers classified on types of bonding generally carried out [59]

Common Types	Cross-linkers	Molecular Structure
(A) Covalent.	(1) triallyl isocyanurate (TAIC); (2) bis(1-(tert-butylperoxy)-1-methylethyl)-benzene (BIPB); (3) dicumyl peroxide (DCP);	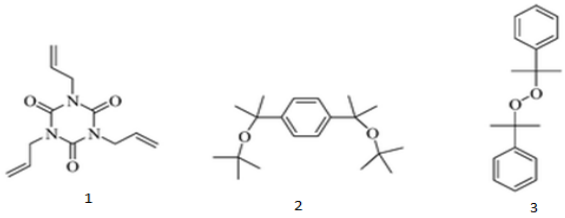
(B) Non-covalent	(4) ethylene glycol dimethacrylate (EGDMA); (5) N,N′-methylenediacrylamide (MBAA); (6) divinylbenzene (DVB)	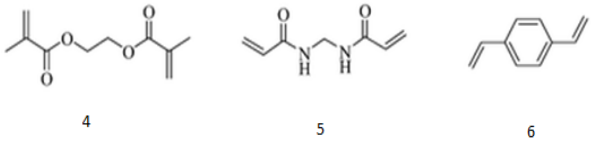

It is reported in the literature that the best interaction between monomer and template occurs when there is complementarity, and the monomer with acid functional groups reacts with template with basic functional groups and vice-versa.[58] In all molecular imprinting processes the template molecule plays a central role since it directs the organization of functional groups of the monomers. Complementarity interactions between the template molecule, functional monomer and crosslinking agent are necessary to create a molecular organization.

In fact, for all this to occur, a porogenic solvent must be chosen to promote the solubilization of the reagents, allowing the interactions between template and monomer to occur efficiently, thus contributing to the formation of a MIP with high porosity. Thus, the evaluation of the functional groups of the monomers and the template is important for choosing the best monomer for the synthesis. It should also be understood that the maximum efficiency of the

formation of the impression occurs when the polymerization reaction is performed using an appropriate solvent so that the solubility of the printed species is not compromised.

The porosity of the MIP will depend on the degree of solubility of the reactants, because the lower the solubility, the larger the non-selective pores and the low surface area will form. When high solubility occurs, small pores, the size of the target molecule, and large surface area will form.

The rigidity of the template in the MIPs is performed using a crosslinking reagent or crosslinking agent, the most commonly used being ethylene glycol dimethacrylate (EGDMA), which must be in excess during the polymerization, generally following a ratio with the template from 1:20 to 1:200 (mol/mol). The crosslinking agent used in obtaining an MIP performs many functions such as control of polymer matrix morphology, stabilization of binding sites with molecular recognition ability and stabilization mechanical properties of the polymer matrix. During synthesis has been used a high amount of crosslinking agent, so that not only obtain macroporous materials such as mechanically stable materials also possible to maintain the complementary three-dimensional structure. Accordingly, the functional groups will be in an optimal configuration for the re-assembly of the template molecule, allowing the recipient to recognize the original substrate and consequently the high specificity of the polymer. As a rule, the polymers have grading degrees greater than 80%.

The polymerization reaction begins with the use of a radical initiator under heating that can occur with the use of a water bath or UV radiation in the absence of oxygen. The best-known radical initiators given in Table 3 are: (AIBN)2,2'-azo-bisisobutyronitrile, (ABDV) azo-bis-dimethylvaleronitrile, benzoyl peroxide (BPO) and 4,4'-aza-*bis*-(4-cyano pentaenoic acid).

Table 3: Common polymerization initiators used in the synthesis of MIPs[59]

Initiators	Molecular Structure
(1) Azobisisobutyronitrile (AIBN); (2) azobisdimethylvaleronitrile (ADVN); (3) 4,4′-azo(4-cyanovaleric acid) (ACID); (4) benzoylperoxide (BPO); (5) dimethylacetal of benzyl (BDK); (6) potassium persulfate (KPS).	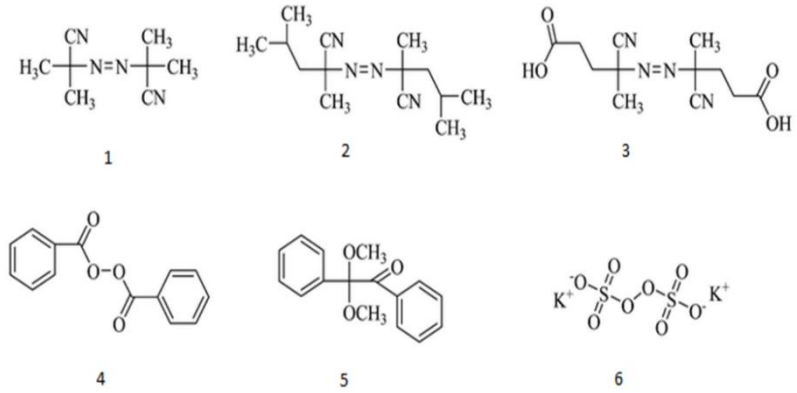

Polymerization of MIP involves three important steps: initiation, propagation and termination.

Initiation: Once the formation of the polymer chain is initiated, it propagates in a short time (possibly one or two seconds), giving rise to a high molecular weight molecule before the termination process occurs, even when the amount of monomer consumed is low. Normally, the initiator promotes the formation of free radicals by remaining active throughout the polymerization process. Many initiators, with different chemical properties, can be used as source of radicals in polymerization processes. Usually, their concentration is low in comparison to that of the monomer, for example, 1% relative to the total number of moles of polymerizable double bonds[60].

The initiation is accomplished by homolytic cleavage yielding two active free radicals, followed by the double bonds in the monomer that react with the unpaired electrons of the radical. In this reaction, the active center of the radical strikes the double bond of the monomer or the crosslinking agent, leaving an unpaired electron in the monomer as a new active center.[61,62]. The activation of this reaction is usually carried out by thermal decomposition or photolysis. Below we have a simplified scheme of the reactions performed in this step, where is represent the initiator, R the activated radical of the initiator, M the monomer and M the activated monomer.

$$I \longrightarrow 2R^{\bullet} \qquad \text{(reaction 1)}$$

$$R^{\bullet} + M \longrightarrow M^{\bullet} \qquad \text{(reaction 2)}$$

Propagation: After initiation, the growth of the polymer chain occurs at a very rapid propagation rate. The polymer chains increase significantly reaching a high molecular weight at the end of this step.[63]

Termination: The termination occurs when the polymer terminates the growth through free electrons of two growing chains that join together and form a single one. In the scheme below C_a and C_b represent growing chains active, and C ab the final chain after the termination process.

$$\mathbf{C_a + C_b \longrightarrow C_{ab}} \qquad \text{(reaction 3)}$$

1.3 Core-shell Magnetic Molecularly Imprinted Polymer

Preparation of the polymer with the selective character (as previously described selectively adsorb analyte), MIPs demonstrate advantages in terms of adsorption capacity, chemical stability and reproducibility. In view of these advantages, the immobilization of MIPs on various surfaces of solid supports, such as core@shell[64], nanowire[65], optical fiber[66], electrodes[60] have been reported. The development of chemical sensors, becoming more interesting. In this way, the MIP will act as the sensing phase conferring high selectivity to the system. In addition, to being possible to perform extractions, pre-concentrations and clean-up samples in a sensitive way.[67]

Nanoparticles are solids up to 100 nm in size and have characteristics of high surface area in relation to its volume.[68] These nanoparticles are mostly used as nuclei for the MIP core@shell. Among these, iron oxide magnetic nanoparticles with superparamagnetism and high stability is the best choice materials.[69] [70] The most commonly reported synthesis of magnetite methods being coprecipitation,[71] hydrothermal,[72] sonication and polyol. Co-precipitation is widely used easy and fast method; salts of iron (II) chloride and iron (III) precipitated in alkaline medium to form magnetite.[73]

Among several advantages presented, the principal is its surface characteristics that allow its easy encapsulation and modification to protect them from degradation, while preserving their magnetic response.[74] The modification of the magnetic cores became necessary prior to polymerization, to avoid loss of the polymer layer around magnetic cores. Silanizing agents, such as tetraethylorthosilicate (TEOS) extensively applied to the magnetite coating by the sol-gel method.[75] Thus high density silane layer of terminal functional groups is achieved, allowing various types of covalent coupling on its surface, reducing the leaching problem of the polymer layer.

In analytical separation magnetic MIP is applied directly to the sample, without the need for previous treatment of the same. In addition, the polymer is readily separated from the test solution by the application of an external magnetic field, such as a magnet.[76]

Magnetic MIPs have been recently employed for several complex matrices such as river waters containing different contaminants – dyes, antibiotics, herbicides, using spectrophotometry, liquid chromatography, HPLC as well as electrochemical detection methods.

1.4 Kinetic studies in MIPs

One of the ways to evaluate MIP binding sites is through kinetic studies that rely on an adsorption study of the template in MIP at certain time intervals. In this method, a fixed amount of MIP is brought into contact with solutions containing different amounts of caffeine for a specific analysis time. After contact for any given time, the solution is separated from the polymer by filtration. Next, the solution is used to measure the concentration of free (remaining) template molecule and is determined by reference analytical methods (such as HPLC-UV) and by difference the amount bound (adsorbed) in the MIP. In this type of study, it is possible to find the best adsorption time of the template in the polymer.

1.4.1 Adsorption isotherms obtained for template affinity studies with MIP

Adsorption isotherms are used to determine the maximum amount of template adsorbed on the surface of adsorbent materials (MIP and NIP in this case) at a constant temperature, in order to determine parameters associated with adsorption.

There are several mathematical models for adjusting the experimental data of the adsorption of an analyte to the adsorbent support (isotherms), among them the Langmuir and Freundlich.

One of the characteristics of the Langmuir isotherm is to assume the formation of a monolayer on the adsorbent material and assume an approximation of the adsorption limit quantity (Equation 1).[77,78].

$$q_e = \frac{K_L \times C_e}{1 + a_L \times C_e} \qquad (Equation\ 1)$$

Where: q and is the amount of adsorbed template at equilibrium (mg g^{-1}), C_e corresponds to the template concentration at equilibrium (mg L^{-1}), K_L and a_L are constants in the Langmuir isotherm.

The Langmuir equation can also be represented by the linearized form (Equation 2), which is used to obtain the parameters of this adsorption model.

$$\frac{C_e}{q_e} = \frac{1}{K_L} + \frac{a_L}{K_L} C_e \qquad (Equation\ 2)$$

The Freundlich isotherm, on the other hand, assumes the existence of a multilayer adsorption and predicts an exponential distribution of several adsorption sites with different energies. It is represented by Equation 3: [77,78].

$$q_e = K_F \times C_e^{b_F} \qquad (Equation\ 3)$$

Where: q e is the amount of template adsorbed at equilibrium (mg g^{-1}), C_e is the concentration at equilibrium (mg L^{-1}), K_F and b_F are parameters corresponding to the Freundlich isotherm. The linear form of the Freundlich equation is given by Equation 4: [77,78].

$$\ln q_e = \ln K_F + b_F \ln C_e \qquad (Equation\ 4)$$

1.5 Application of Molecularly Imprinted Polymers (MIP)

The solid phase extraction method (SPE) is a widely used method for the extraction, clean up and concentration of analytes when they are present at low concentration levels. Through this methodology it is possible to carry out the removal of the analyte of interest, separating it from interfering compounds in complex matrices. Therefore, SPE is considered a very important method for the preparation of samples.

The use of MIP as adsorbent material in the solid phase extraction technique has been shown to be of high selectivity and chemical and thermal stability when compared to other materials such as modified silica (C18), ion exchange resins and immunosorbents, besides reproducibility in the preparation of the polymer. The technique is referred to as solid phase extraction with molecular imprinting (MISPE). MISPE functions as a conventional SPE procedure, except for the substitution of common stationary phases for the printed polymer. Thus, it comprises the steps of conditioning, loading, washing and eluting the cartridges.[78].

Initially it should be considered that the solvent in which the samples are to be percolated should not interfere in the interactions formed between the polymer and the analyte in order that the retention of the analytes is the largest possible. The characteristics of the analyte used as a template are important for the choice of the best washing solvent. They are usually used low polar solvents such as dichloromethane, toluene and chloroform or high polar solvents such as methanol. Thus, in this type of analysis the conditions of pH, polarity and volume of solvent must be optimized, so that the template separation of the interfering compounds is made. The efficiency of this method as well as the applicability of this material in different matrices will depend on several factors, such as amount of MIP used, MIP efficiency in adsorption, interaction of the template with the active site and the way the analysis is performed.

Thus, this thesis was aim to develop a MMIP selective to caffeine and its application in various methods and techniques, for caffeine analysis in quality control labs for different market samples and food items, containing caffeine and, also for online on spot analysis of environmental studies.

2 Objective

The main objective of the work is the synthesis and characterization of Magnetic-MIP (MMIP) for Caffeine, and its evaluation as recognition system, aiming at in the future the development of chemical sensors for application in different matrix.

The optimization of the synthesis and characterization of MMIP for caffeine, thus includes investigation of the interaction between the caffeine and the functional monomers used for MIP synthesis, evaluation of reagent quantities and the method used for MIP and MMIP synthesis, affinity studies between MIP and analyte, and spectrophotometric determination of caffeine using MMIP.

3 Material and Methods

3.1 REAGENTS AND SOLUTIONS

The reagents used for magnetic-MIP synthesis (MMIP) were caffeine (CAF), methacrylic acid (MAA), acrylonitrile (AN), ethylene glycol dimethacrylate (EGDMA) and 2,2'-azo-*bis*-2-methylpropionitrile (AIBN), trimethylolproprane trimethacrylate (TRIM), ethanol and acetonitrile all provided by Sigma-Aldrich®. Solvents used for synthesis and removal of the template molecule were methanol (Panreac®) and glacial acetic acid (Synth®), deionized water (MilliQ®) and acetonitrile (Panreac®).

For synthesis and modification of the magnetic nanoparticles the reagents were $FeCl_2.4H_2O$ and $FeCl_3.6H_2O$ (Sigma-Aldrich®); NH_4OH (Synth®); tetraethylorthosilicate (TEOS) from Acrois®; 3-(trimethoxysilyl)-propyl-methacrylate (MPS) Sigma-Aldrich®, ethanol and toluene, both provided by Synth®. Theophylline (THP) and xanthine (XTN) (Sigma-Aldrich®) were used for selectivity studies.

3.2 INSTRUMENTATION

In order to evaluate the physical characteristics of the synthesized materials, a series of physical characterizations were performed.

Spectrophotometric measurements were performed on an UV/vis spectrophotometer (Bel Tech model). The measurements in solution were made using 1.0 cm quartz cuvettes of optical path, in the range of wavelengths 190 to 400 nm. The absorbance measurements in solution performed for the evaluation of the immobilization of the MIP over magnetic nanoparticles.

To carry out the pH measurements, was used a pH-meter of the brand Digital Gehaka® model PG 2000. The vacuum pump used is EIKONAL® (Model 131/132).

Millipore® Milli-Q Ultra-Pure Water System was used to obtain ultrapure water used in all thesis.

The spectra in the infrared region were obtained by employing an absorption spectrophotometer in the middle infrared Fourier transform (Fourier-Transforming infrared spectroscopy-FTIR) VERTEX 70 of Bruker®. For the Spectra collection, 64 sweeps were

performed between the range 4000 to 400 cm^{-1}. The spectra were obtained by the total attenuated reflectance technique (ATR), using Diamond crystal.

The morphology of the nanoparticles and polymers was analyzed using transmission electron microscopy (TEM), performed by the Phillips CM 200® branded equipment, operating at 200 KV, LaB6 filament. The samples were prepared over Copper grids (TED Pella®, ultrathin C type A, 400 mesh). The materials were dispersed in isopropanol and kept in ultrasound for 10 minutes for its redispersion. 2 mL of the suspension was dripped into the copper grille, which was dry at room temperature for the performance of the analysis.

Magnetometry is a method used in order to determine the magnetism of a material when subjected to the application of a magnetic field. The classical form of analysis is by means of the measure of attraction or repulsion of the material by a magnetic field. The Equipment Lakeshore VSM® 7300 series was used for magnetic characterization. The measures were performed by Dr. Luis Alvares, researcher at the Bariloche Atomic Center, Magnetic Resonance Division, Argentina.

3.3 CHROMATOGRAPHIC METHOD

Liquid chromatograph (HPLC) Shimadzu® brand, which has the following components: UV-Vis detector (SPD-model 20A), auto-sampler (SIL-20A), pump (model LC-20AT) and interface (model CBM-20A). For this, was using a Zorbax SB-C18 column of Agilent® in the dimensions 150 mm X 2.4 mm, flow of 1 mL min^{-1}, room temperature, wavelength 274 nm absorption and mobile phase consisting of 60% of water and 40% of metanol isocratic mode. All reagents used were of analytical purity. (Caffeine USP Monograph with little modification)

An analytical curve was built in order to evaluate the retention time of caffeine in the concentration range of 1.00 to 200 µmol L^{-1}. The solutions were filtered on filters of regenerated cellulose (RC) with 0.45 µm pore diameter and volume 20 µL injection.[79]

3.4 COMPUTATIONAL SIMULATION

To obtain highly selective MMIPs, the interaction between the functional monomer and the template molecule is one of the crucial factors to determine theoretically, the satisfactory synthesis of these materials. In this way, the simulations carried out focused on obtaining the information that indicated the greater affinity between the Template and several monomers commercially available and that are commonly used in the synthesis of MIP for different analytes, for this, the following programs were used:

1. *HyperChem® 8.0.5*: Used for Molecular modeling to be used in the synthesis of MIP.
2. *OpenEye®* (software package) containing the programs:
   - LIFE 3.0.0: Used to visualize the modeled molecules and to check for possible link errors between atoms.
   - Omega2: It generates diverse conformers of the molecules, which makes possible to take into account possible spatial impediments. By default, 10 conformers are generated, 3 randomly chosen to perform the simulator tests.
   - Szybki 1.2.2: Program that takes the molecule to its lowest energy state and therefore more stable.
3. *AutoIt 3.3.6.0*: An application that uses command lines (scripts) to automate repetitive processes during molecular modeling, eliminating human errors during procedures.
4. *Multiple Minima Hypersurfaces* (MMH) with MOPAC (Molecular Orbital PACkage) 2009: Used to perform the simulations themselves. This program approaches the monomers with the molecule that will use as a template by calculating the energy released, thus resulting in the affinity between them.

MOPAC is a utility that employs semi-empirical quantum chemistry for approximation calculations

The 20 monomers shown in Table 4, which were named MP1 to MP20, were evaluated for simplicity of analysis of the results.

Table 4: Monomers commonly used in the synthesis of MIP and chosen to perform the computational simulation[60].

Sign	Monomer	Sign	Monomer
MP1	bis-acrylamide N,N-methylene	MP11	Methylenesuccinic acid
MP2	acid imidazole-4-acrylic	**MP12**	**methacrylic acid (MAA)**
MP3	Ethyl imidazole-4-acrylic acid ester	MP13	divinylbenzene 3
MP4	Acrylic acid	MP14	divinylbenzene 4
MP5	Acrylamide	MP15	Styrene
MP6	Acrolein	MP16	Vinylimidazole
MP7	Allylamine	MP17	Vinylpyridine
MP8	**Acrylonitrile**	MP18	Vinylpyridine
MP9	**Ethylene glycol dimethacrylate**	MP19	2-acrylamide-2-methyl-1-propane-sulfonic
MP10	(Cianoetilamino)-ethyl methacrylate	MP20	2- hydroxyethyl methacrylate

Source: adapted from Wong, A., 2015.[60]

Three functional monomers are selected as blue in the table above because of the simulation results obtained for these functional monomers. From the simulation results graph it is clear that MAA had higher biding energy, AN had medium binding energy while EGDMA has the lower level in binding energy curve as shown in Figure 3.1.

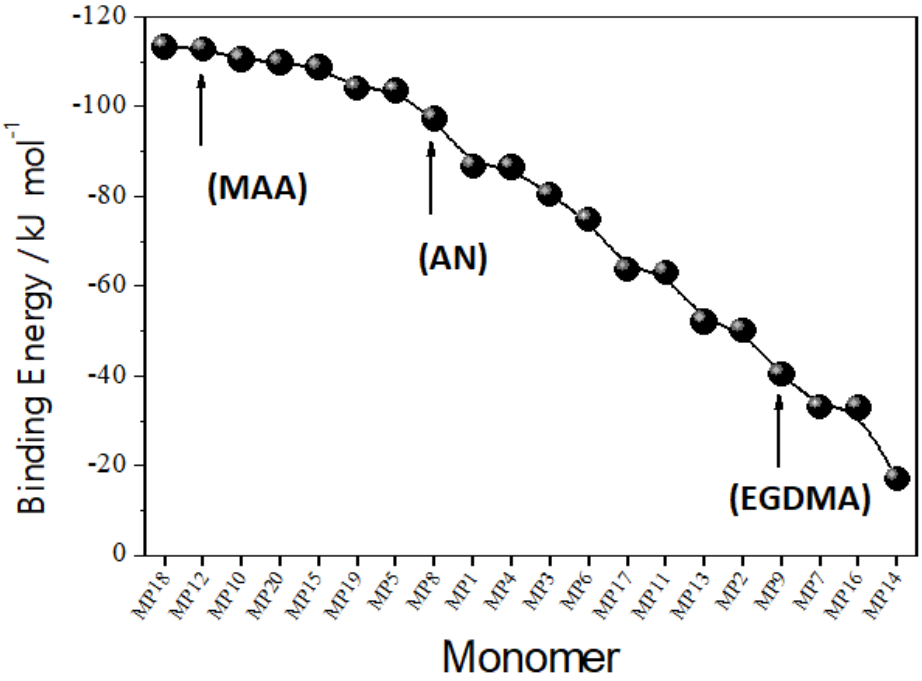

Figure 3-1: The simulations evaluate the energy of the interaction caffeine with the 20 monomers proposed in Table 4.

Source. Own uthorship

3.5 EXPERIMENTAL PROCEDURES

3.5.1 Synthesis of magnetite nanoparticles

The procedure for the synthesis of magnetite (Fe_3O_4) is based on the presented by Ben Aissa et al.[80] and Figure 5 briefly shows the experimental procedure. Thus, co-precipitation of 0.01 mmol Fe^{2+} and 0.02 mmol of Fe^{3+} in basic medium. For this, the iron salts were added to a beaker in 80 mL of H_2O deionized and 10 mL of NH_4OH was added, drop by drop, using a Pasteur pipette. The pH of the mixture was held at 9.0 and the reaction was carried out for 30 minutes. After the reaction have been finalized, magnetite (Fe_3O_4 core) was formed. The precipitate was then separated from the supernatant using a neodymium magnet and, finally, filtered and washed with water until pH 7 and dried in vacuum desiccator by 12 h.

Then, in order to prepare the magnetic material for future modification with the MIP, the magnetic nanoparticles have been modified by means of the sol-gel process with TEOS (*orto*-silicate of tetraethyl). This procedure allowed the covering of magnetic nanoparticle with silanes, forming a glassy surface on the magnetic material for subsequent silanization. For that, it was heavy 300 mg of Fe_3O_4, which was dispersed in 4 mL of absolute ethanol and 4 mL deionized H_2O, and sonicate for 30 min. Then, 5 mL of TEOS were added the suspension of magnetite, leaving react by 12 h at room temperature under constant mechanical agitation, thus forming $Fe_3O_4@SiO_2$. Finally, the product obtained was washed and filtered with ultrapure water, and dried in vacuum desiccator for 12 h.

In the subsequent step, silanization of magnetite-TEOS ($Fe_3O_4@SiO_2$) has been carried out. For this, weighed 250 mg of $Fe_3O_4@SiO_2$, which were dispersed in 5 mL of toluene, followed by the addition of 5 mL of MPS (3-(trimetoxisil) propyl methacrilato). The reaction was performed by 12 h under mechanical agitation and constant stream of N_2. Finally, the silanized material (named $Fe_3O_4@$ SiO_2-C=C) was filtered and washed with ethanol, dry in vacuum desiccator for 12 h.

The procedure of synthesis and modification of magnetic nanoparticles are schematized in Figure 3.2.

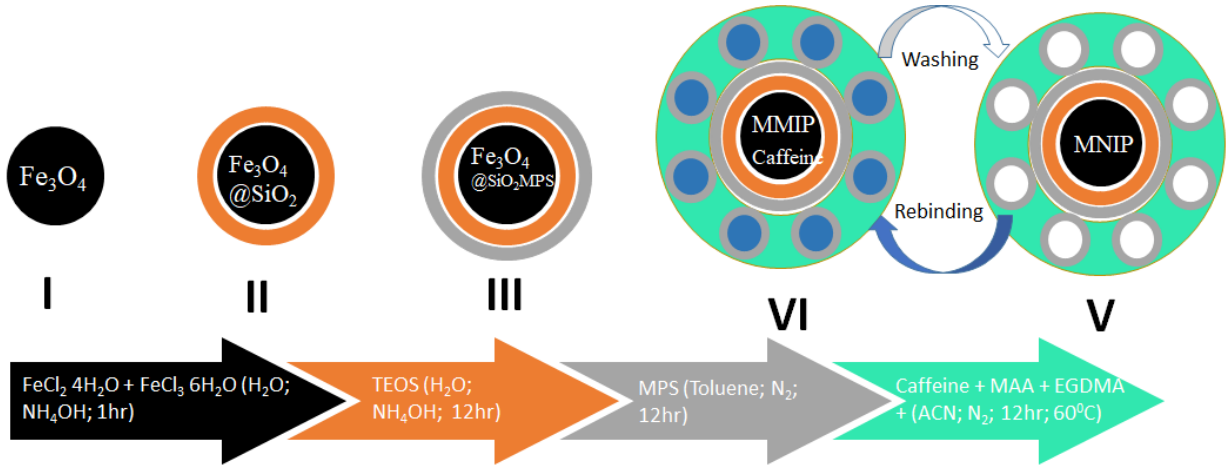

Figure 3-2. Synthesis and modification of magnetite nanoparticles I, II, III.
Source. Own authorship

3.5.2 Synthesis of magnetic MIP

The synthesis of magnetic MIP for caffeine by the non-covalent method has been optimized. Simplified, the procedure adopted was the synthesis by precipitation and bulk polymerization given in Figure 3.2 each specific monomer and template (caffeine) were mixed and allowed to interact for 1 hours at 25 °C (Figure 3.3). Next, modified magnetite nanoparticles were added and the system under constant agitation for 2 hours in sonication bath. Finally added to the mixture was EGDMA and AIBN (radical initiator). N_2 was bubbled continuously in the solution in order to prevent oxygen from interfering with the polymerization. Finally, the system was heated to 60 °C for 24 h.

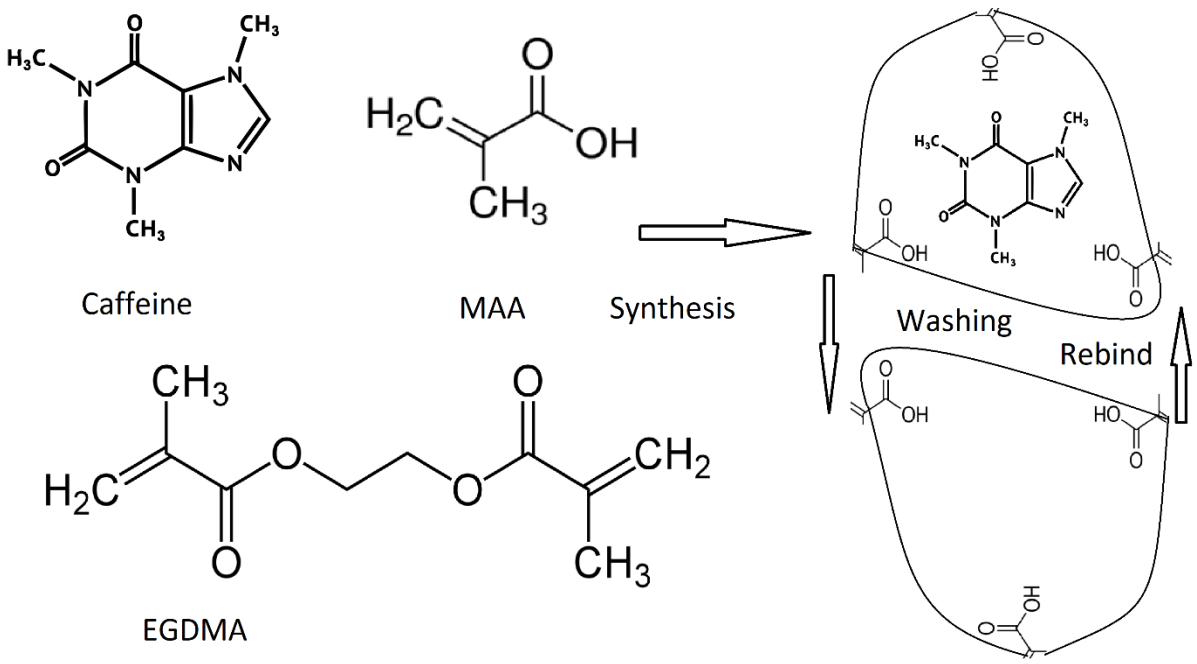

Figure 3-3: Schematic representation for the synthesis of MIP for caffeine.
Source. Own authorship

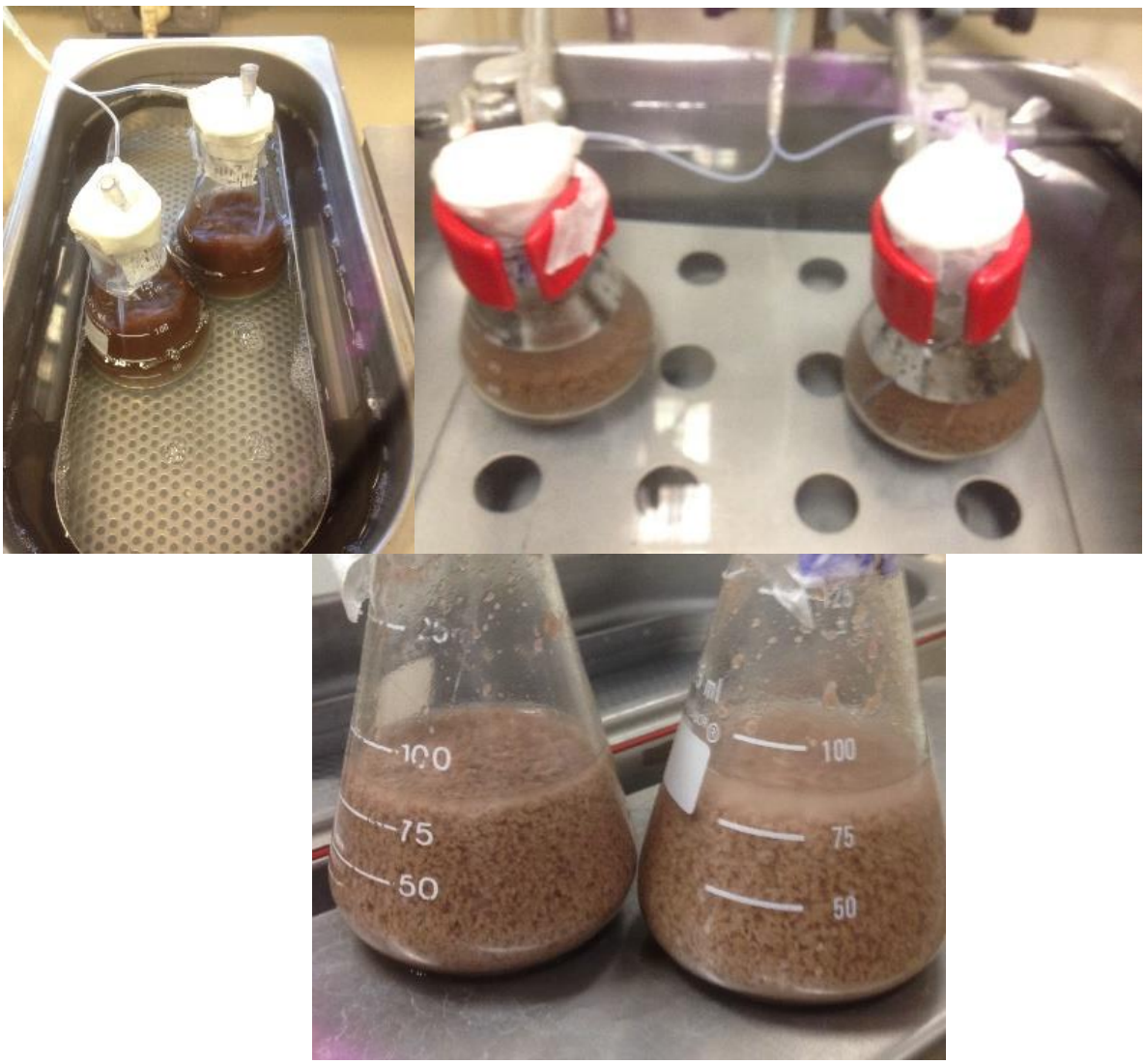

Figure 3-4: Photography of the system used in synthesis of MMIP for Caffeine and the respective MNIP.

Source: Own authorship

The amounts of reagents used for each type of MMIP and MNIP synthesized in this work are given in Table 5.

Table 5: Reagent amounts used for the different MMIPs and MNIPs synthesized in this work.

Item	Template: Caffeine / mg	Functional Monomers: MAA, EGDMA, ACN (volume in µL)	Solvent: EtOH or Acetonitrile (mL)	MNPs Fe_3O_4 (mg)	Crosslinker: EGDMA, TRIM (volume in µL)	Initiator AIBN (mg)
MMIP 01	20	**MAA 70**	30	200	**EGDMA 390**	8.2
MNIP 01	0					
MMIP 02	20	**EGDMA 155**	80	200	**TRIM 27**	8.2
MNIP 02	0					
MMIP 03	20	**ACN 55**	80	100	**EGDMA 390**	8.2
MNIP 03	0					
MMIP 04	20	**MAA 70**	30	200	**TRIM 27**	8.2
MNIP 04	0					
MMIP 05	20	**EGDMA 155**	30	100	**TRIM 27**	8.2
MNIP 05	0					
MMIP 06	20	**ACN 55**	30	100	**EGDMA 390**	8.2
MNIP 06	0					
MMIP 07	40	**MAA 136**	**Acetonitrile** 30	200	**EGDMA 770**	8.2
MNIP 07	0					

Source: Own authorship.

To finish the synthesis, the polymer was separated by magnet and washed with methanol/water to remove caffeine and reagents in excess followed by vacuum filtration. The complete cleaning was done by soxhlet extraction Figure 3.4 using first methanol with acetic acid (90:10 v/v), then deionized water for several batches and acetonitrile at final stage each 100 mL for 8 to 12 hours. Along with UV spectroscopic monitoring.

Analogously to the MMIP, MNIP were synthesized, without adding template as control material.

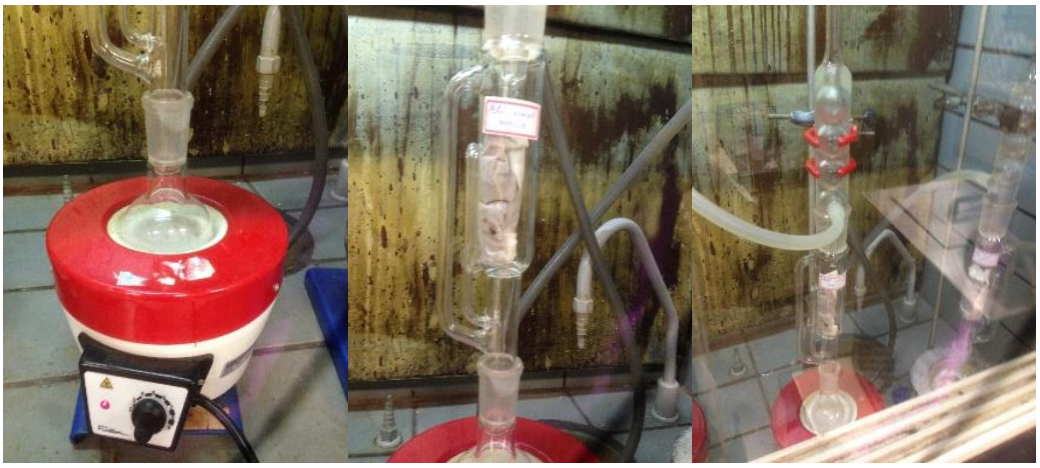

Figure 3-5: Photography of the Soxhlet system used for cleaning of MIPs and NIPs (Left: Solvent heating evaporation. Middle: washing polymer. Right: Vapor condensation.

Source: Own authorship

After the washing step it should be noted that there are no excess reagents as functional monomers in the polymer. It is expected that the number of non-specific links are greatly reduced, since the functional groups that define the recognition sites are theoretically linked to the template.

It is worth remembering that the choice of monomers was based on the computational simulations. In this study, a monomer with high (methacrylic acid) and another with low of monomer-analyte (acrylic acid) binding and medium energy monomer (EGDMA) was chosen.

3.5.3 Study of adsorption kinetics of molecularly imprinted polymers

In this study, 1 – 10 mg of MIP and NIP were pre-weighed and transferred into capped vials and added to a volume 1 – 5 mL having concentration of 5 – 700 mgL^{-1} caffeine solution, the solutions being prepared in various v/v solvents. The vials were sealed and stirred for a specific time in a homogenizer. The time intervals were: 10, 15, 30, 60, 90, 120, 180, 240 minutes. Up to 24 hours. At the end of this period, aliquots of the supernatant were collected and analyzed in HPLC-UV.

3.5.4 Adsorption isotherms

Quantities of 2 – 5 mg of MIP and NIP were pre-weighed and transferred into capped vials and added in a volume of 1 – 5 mL of caffeine solution of concentrations between 10 – 180 ppm. The vials were sealed and shaken for a time interval of 180 minutes (Figure 3.5). At the end of this period, aliquots of the supernatant were collected and analyzed in the UV-Vis Spectrophotometer and HPLC-UV. The amount of substrate that remained free in solution was determined by analysis and the concentration adsorbed by MMIP (adsorbed substrate concentration/g of polymer) is determined by subtracting the initial amount of substrate in the solution (Equation 5).[81]

C ppm polymer adsorbed = C ppm Total - C ppm HPLC (Equation 5)

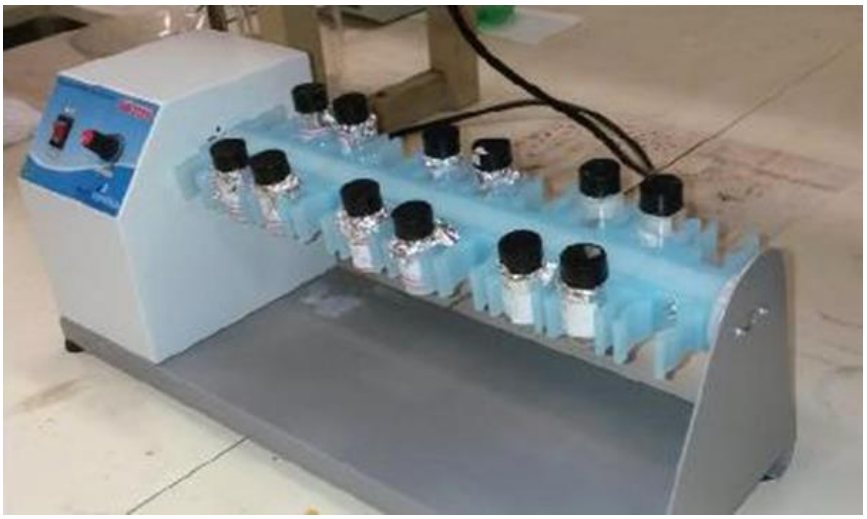

Figure 3-6: Photography of the homogenizer used in MIP/template reconnection assays.
Source: Own authorship

3.5.5 Optimization of Spectroscopic conditions for Caffeine analysis

Caffeine solutions were prepared in methanol, dichloromethane and deionized water. The concentration of caffeine first analyzed for optimization, from 2 – 20 mg L^{-1} in MeOH and water

at 278 – 274 nm maximum wavelength respectively, calibration curve was plotted for this concentration range.

3.5.6 Studies of optimization and evaluation of the efficiency of polymers

To evaluate the adsorption capacity by magnetic MIP and NIP polymers synthesized, were weighed into Eppendorf® tubes amounts of these materials in a range of 0.5 to 5.0 mg and mixed with 1.0 mL of 10.0 mg L^{-1} caffeine solution during 2 h under gentle mechanical shaking. After the time has elapsed, the MMIP was magnetically separated by external magnet, the solution was analyzed by UV-Vis spectrophotometer.

The amount of MMIP and MNIP were decreased in the successive experiments from 25 mg mL^{-1} to 1.0 mg mL^{-1} for obtaining better results.

3.5.7 Evaluation of solvent, mass dosage and time

Optimization studies began with a preliminary solvent for caffeine rebinding. For this, 10.0 mg of polymer were interacted with 5.0 mL of 10.0 mg L^{-1} caffeine solution prepared in different solvents: water, methanol, and dichloromethane for 2 hours. At the end of the interaction time, the samples were filtered and analyzed by UV-Vis spectrophotometry (UV-Vis). For the evaluation of the best mass quantity for analysis, a study was carried out in which it was weighed in different glass tubes polymer amount, from 1 – 10 mg. These masses were used to interact with 10.0 mg L^{-1} Caffeine solution prepared in a first moment in methanol and finally in deionized water. After the interaction time, the polymer was separated using a neodymium magnet and filtered solutions are taken for analysis by UV-Vis. After the best polymer mass was defined for the studies, the interaction time were evaluated. Initially 10.0 mg of MIP were interacted with 10.0 mg L^{-1} of caffeine solution prepared in methanol for different times; 10 – 300 min, and in the last experiments 2.0 mg MIP with 20 mg L^{-1} analyte in deionized water for 120 min. After the interaction times were over, the solutions were filtered and analyzed by UV-Vis.

3.5.8 Rebinding and selectivity

In order to evaluate the adsorption capacity of materials MMIP, isotherm curves were constructed. Thus, 10.0 mg of polymer were weighed and interacted under mechanical agitation with different concentrations of caffeine 5.0 mg L^{-1} to 100.0 mg L^{-1} prepared in methanol for initial polymers and, for the MMIP-7 was used 1.0 mg mL^{-1} in 2 mL of water deionized while keep increasing caffeine concentration above 480 mg L^{-1}.

After the interaction time, the polymers were separated with application of a magnetic field (by a magnet neodymium) and the solutions filtered in 0.45 µm PTFE filter and taken for analysis by UV-vis.

The selectivity study was performed in the same manner as described above for the construction of the isothermal curve, being prepared solutions of Caffeine, Theophylline and Xanthine to interact with the polymers.

3.5.9 Application of MMIP in food samples

Caffeine standard solutions were prepared as follow:

Stock solution: 25 mg of caffeine diluted to 25.00 mL (1000 ppm) of deionized water and sonicated for 1 min.

Standard solutions were prepared by diluting 10, 20, 30, 40 and 50 µL of stock solution into 1.0 mL of deionized water, resulting in final concentrations of 10, 20, 30, 40, and 50 ppm.

The samples solutions were prepared as followed:

1. The soda coke: Firstly, were degassed in an ultrasonic bath for 10 min. Then, 40 µL of the drink were diluted until 1.0 mL with deionized water, in order to bring the concentration into the working range of the chromatographic technique.

2. For the analysis of the **Black tea** and **Coffee**, 1.00 g of each sample was weighted and transferred to a 150 mL beaker. To this 50.00 mL of deionized water was added and the solution was boiled for 15 min at hot plate with stirring. The resulting mixture was filtered using Whatman quantitative filter paper. Then 40 µL of the filtrate were diluted to 1.0 mL with deionized water just before the analysis. The dilution processes are summarized in Table 6

Table 6: Dilution chart of beverage samples. Samples diluted nearly to 40 ppm caffeine concentration. Polymer mass 2mg; spread over 120 min in 1.0 mL of an aqueous solution.

Sample	Dilution I	Dilution II
Black Tea	1 g/ 50 mL	40 µL /1 mL
Coffee	1 g/ 50 mL	40 µL /1 mL
Soda coke	40 µL /1 mL	

Source: Own authorship

All samples were acquired in supermarket of the Araraquara city.

For the adsorption experiments, quantities of 2.0 mg of MMIP, MNIP were pre-weighed and transferred into each labeled capped vials and added 1.0 mL of each pre-treatment sample solution. In addition, in order to have an exact value of the caffeine in each sample, 1.0 mL of each sample also was transferred in a vials (Blank) and submitted to the same adsorption process.

After that, the vials were sealed and shaken for 120 minutes. At the end of this period, aliquots of the supernatant were collected and analyzed in the HPLC-UV. [82]

HPLC method employed for analysis of caffeine in these experiments used mobile phase of 40:60 (v/v) methanol/water, column: L1 C18 (150 mm x 4.6 mm, 5.0 µm of particle size), flow rate of 1.0 mL min^{-1} and UV-detector set at 275 nm.

The amount of substrate that remained free in solution was determined by HPLC analysis and the concentration in ppm adsorbed by magnetic polymers were determined by subtracting the remaining free amount of the initial amount of analyte in the blank solutions.

4 Results and Discussion

4.1 COMPUTATIONAL SIMULATION

Using the computer simulation, the interaction of caffeine with the 20 commercial monomers most used for MIP synthesis was analyzed. The purpose of this analysis was to assess the monomers which have greater affinity with caffeine and, thus, to choose the most appropriate functional monomer for synthesis of the MMIP. As a result, a graph is obtained which shows the binding energy between the caffeine and each monomer as shown in Figure 4.1

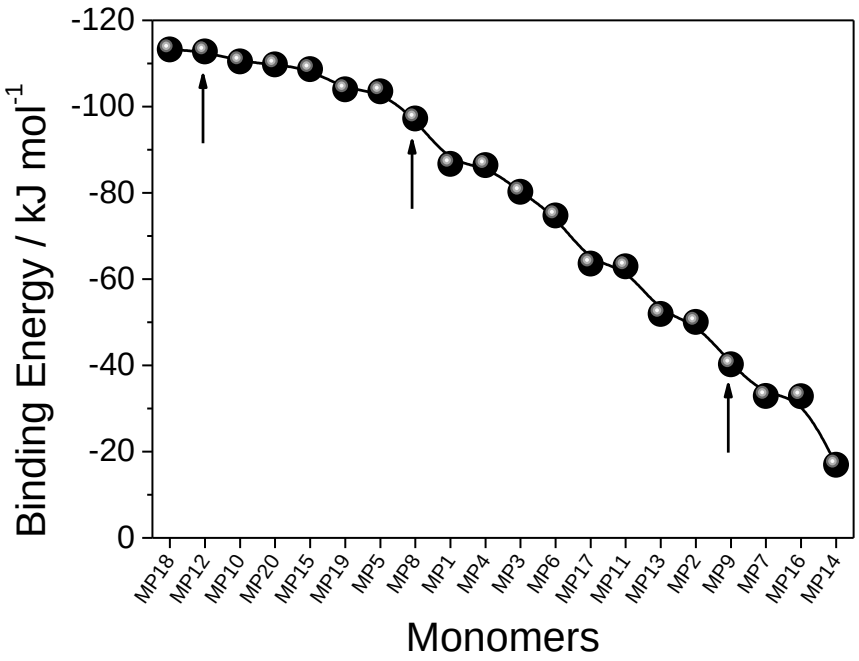

Figure 0-1: The simulation evaluates the energy of the interaction caffeine with the 20 monomers proposed.

Source: Own authorship

The energy values can be understood as the energy released by the rapprochement between caffeine and each of the monomers. In this way, the higher the energy released, the greater the affinity between the two compounds, indicating thereby the monomer that can confer greater selectivity to the MIP.

The functional monomers (FM) chosen for the synthesis of MIPs for caffeine, using the result of the computational simulation are methacrylic acid - MAA (MP 12) a monomer having high interaction energy, acrylonitrile - ACN (MP 8) a medium binding energy with the analyte and lower interaction energy EGDMA (MP 9) monomer. The molar ratio employed in the synthesis was 1:4:20 among Template (T), FM, cross-linker (C), as described in the experimental procedure (Table 5).

4.2 CHARACTERIZATION

Characterization of the materials will be discussed according to techniques used, to facilitate comparison between different syntheses and materials results will be discussed in set for each type of characterization.

4.2.1 Fourier transform infrared spectroscopy (FTIR)

FTIR measures of all syntheses were carried out for comparison and monitoring of different stages of synthesis. Assigned bands basically come from stretching vibrations, or bending vibrations. In addition, each infrared (IR) spectrum.

The most suitable functional monomer used for the synthesis of MMIP is one that will interact with the functional groups of the analyte to form a selective cavity, in this particular case, methacrylic acid. As shown in Figure 4.2 the main bands are OH stretch than occurs between 3100 and 2800 cm^{-1} overlapping the CH absorptions. The stronger absorption at 1700 cm^{-1} can be attributed to the carbonyl group.

Once the EGDMA form the polymeric rigid structure, is the reagent being used in greater quantity, both as MMIP and MNIP after properly cleaned, they show only the bands for the EGDMA, such as shown in Figure 4.3, than show the band at 1715 cm^{-1}, corresponding to ester group.

Figure 4.2 also shows the IR-spectra of the caffeine MMIP 07, MNIP 07, modified magnetic Fe_3O_4 with TEOS, MPS, and original nanoparticles. For silanization step of the nanoparticles TEOS shows a very strong band for the Si-O that appears in the range from 1260 to 980 cm^{-1}. The spectrum of methacrylic acid which appease as an intense peak at 1700cm^{-1} due to esterification of COO group for both MAA and EGDMA. These spectral differences in comparison with reagents and monomers used are showed (Figure 4.1) due to the interaction between template and monomer gave changeable peaks in the MIP spectrum.

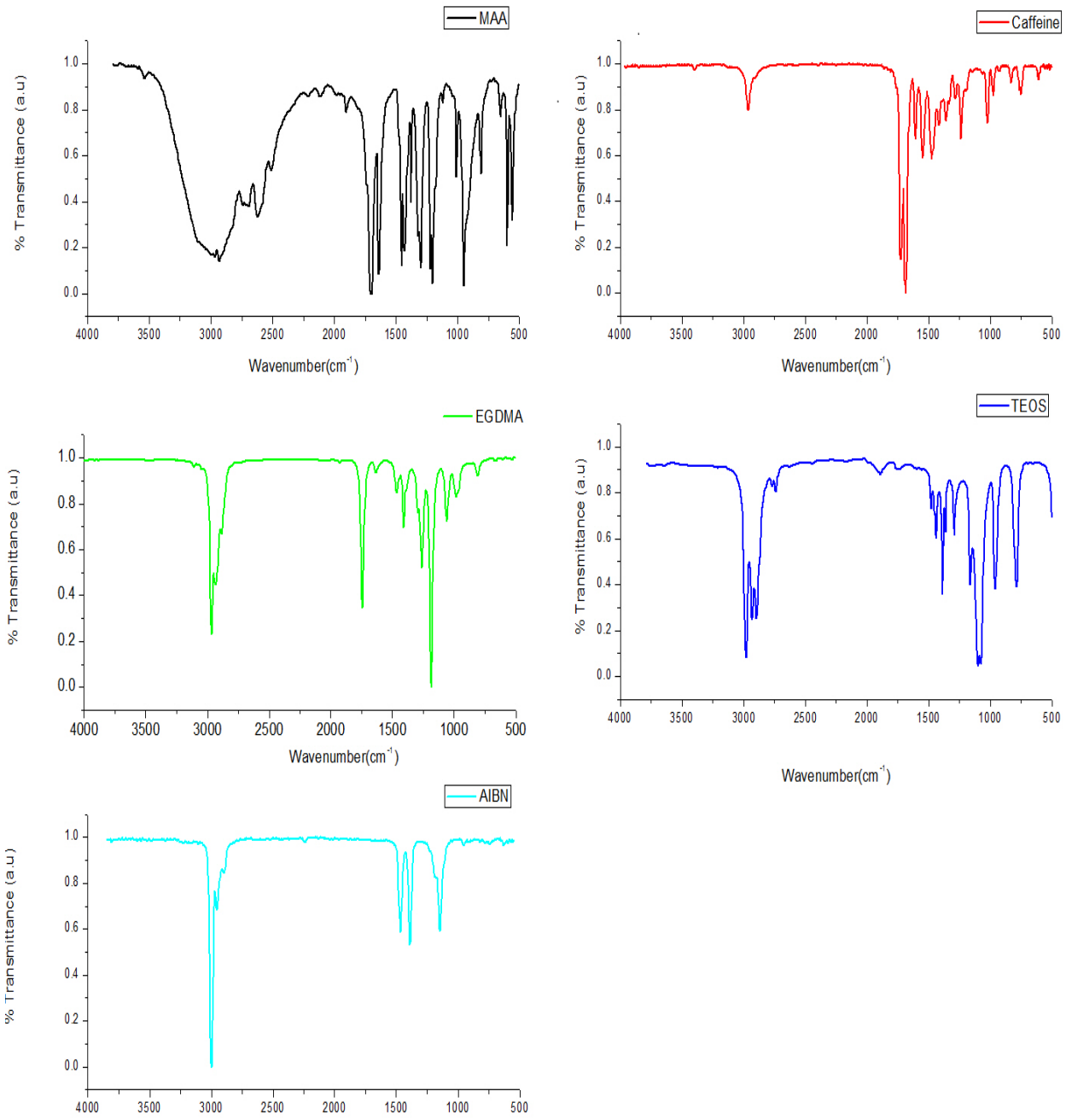

Figure 0-2: FTIR spectrum of methacrylic acid (MAA), Caffeine, EGDMA, TEOS, and AIBN.

Source: Own authorship

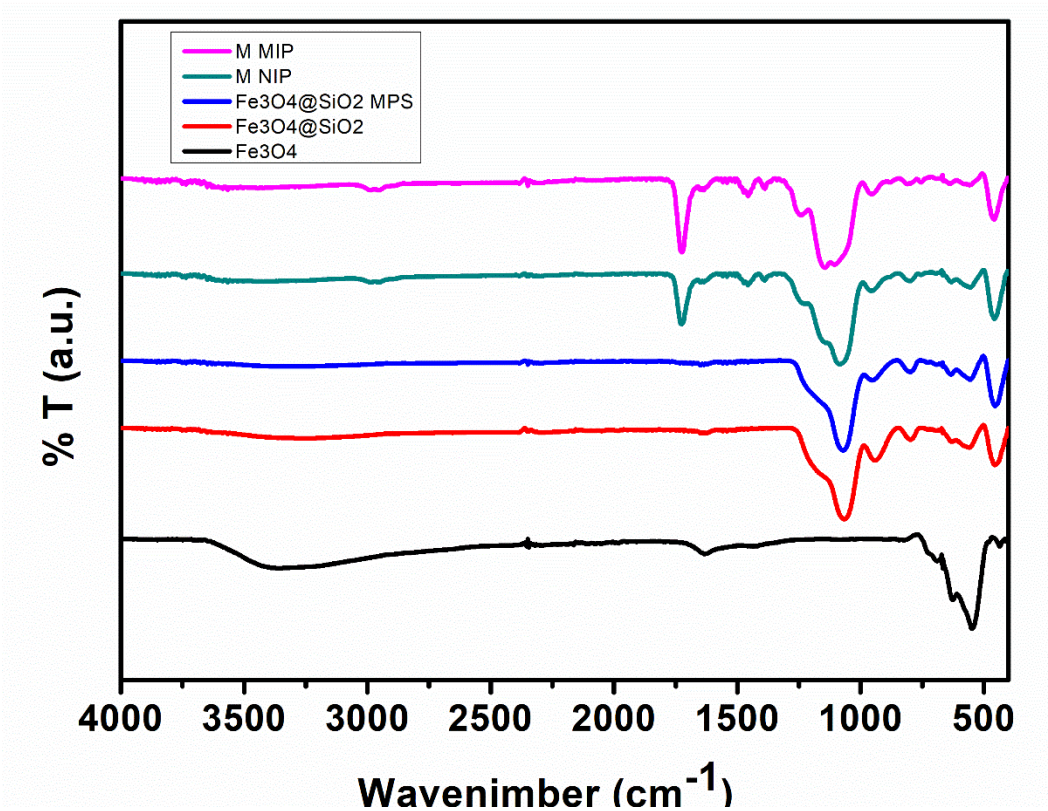

Figure 0-3: Spectrum in the IR region for different stages of synthesis (Fe_3O_4, Fe_3O_4@SiO_2, Fe_3O_4@SiO_2-MPS, MNIP and MMIP).

Source: Own authorship

From the spectra, it is possible to verify the presence of a band at 550 cm^{-1} region assigned to this connection between Fe vibration, is also noticed in Fe_3O_4 nanoparticles covered with TEOS, is observed a suppression of this band in 550 cm^{-1} and the emergence of a band of intense in 1063 cm^{-1}, which is assigned to the vibration of the Si-O bond, showing that there was the formation of glassy layer on the surface of magnetic nanoparticles of iron oxide.

4.2.2 Morphological characteristics

Magnetite synthesis, modification and functionalization and finally achieving MMIP and MNIP increase the diameter of the particles in each successive step. The transmittance electron microscope (TEM) studies of the materials; Fe_3O_4, Fe_3O_4@SiO_2, Fe_3O_4@SiO_2-C=C, MMIP, and

MNIP were analyzed to evaluate morphology, distribution and surface features of these materials. In Figure 4.3, are showed the TEM microscopies to the Fe_3O_4.

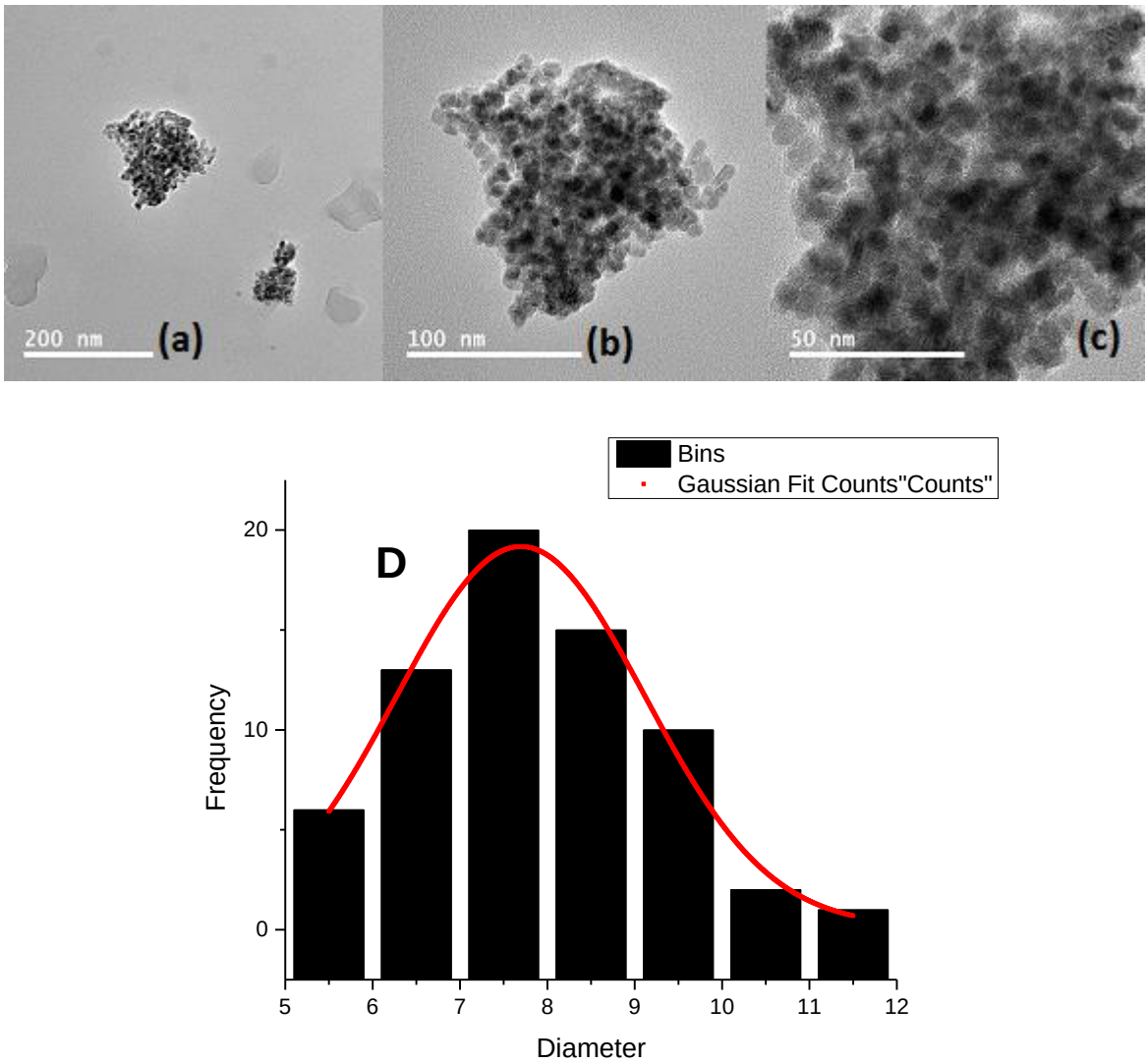

Figure 0-4 ;TEM images of magnetite Fe_3O_4 (a) 200 nm, (b) 100 nm, and (c) 50 nm magnification and (d) size distribution histogram of magnetite.
Source: Own authorship

In the images (a, b, and c) of the Figure 4.3, it can be observed that nanoparticles of Fe_3O_4 presented the formation of agglomerates due to apparently higher paramagnetic attraction among these nanoparticles. Also, it can be observed uniformity in relation to their size, which

can be seen in Figure 13d, that describes the histogram of nanoparticle size distribution and the Log Normal distribution curve. Find the value of medium diameter (d_{med}) of magnetic nanoparticles, which showed a value of 7.7 nm (± 0.1).

The modification of the magnetite with TEOS forming Fe_3O_4@SiO_2 resulting slightly increase the diameter of the nanoparticles, morphology, distribution and surface features (Figure 4.4).

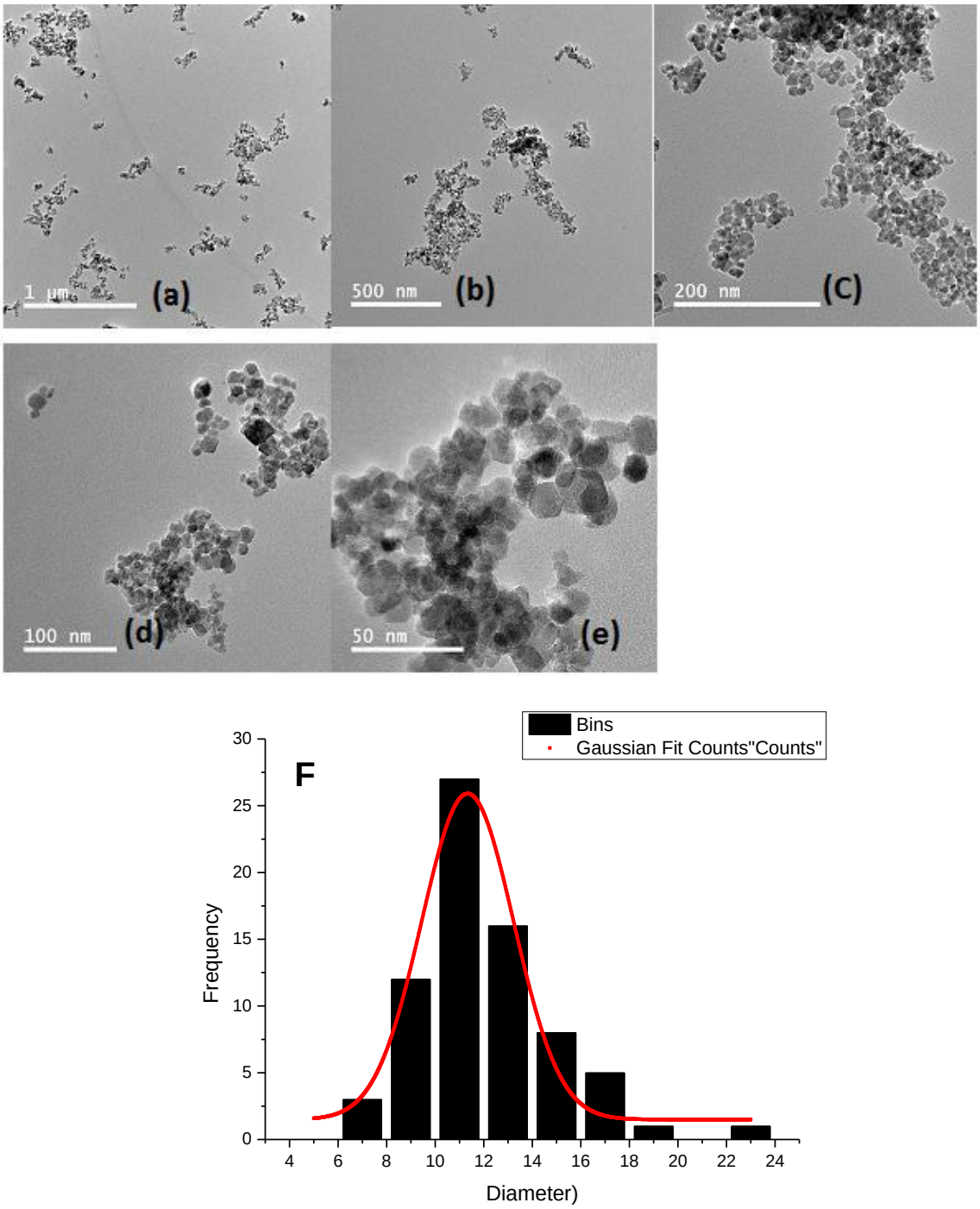

Figure 0-5: TEM images of (a) 1 µm, (b) 500 nm, (c) 200 nm, (d) 100 nm, and (e) 50 nm magnification of Fe_3O_4@SiO_2 and (f) size distribution histogram.
Source: Own authorship

In Figure 4.4 (a, b, c ,d, and e) one can observe images of nanoparticles of $Fe_3O_4@SiO_2$ showing that these still remain agglomerated because the magnetic attraction that they present, however feature a uniform increase in its size, which can be evaluated through Figure 4.4f , which shows the histogram of particle size distribution and adjustment performed using Equation, in this way the Log Normal $Fe_3O_4@SiO_2$ present d_{med} value of 11.3 nm (± 0.2).

Further modification of the magnetite with MPS forming $Fe_3O_4@SiO_2$-C=C resulting slightly more increase the diameter of the nanoparticles, change in morphology, distribution and surface features as shown in Figure 4.5.

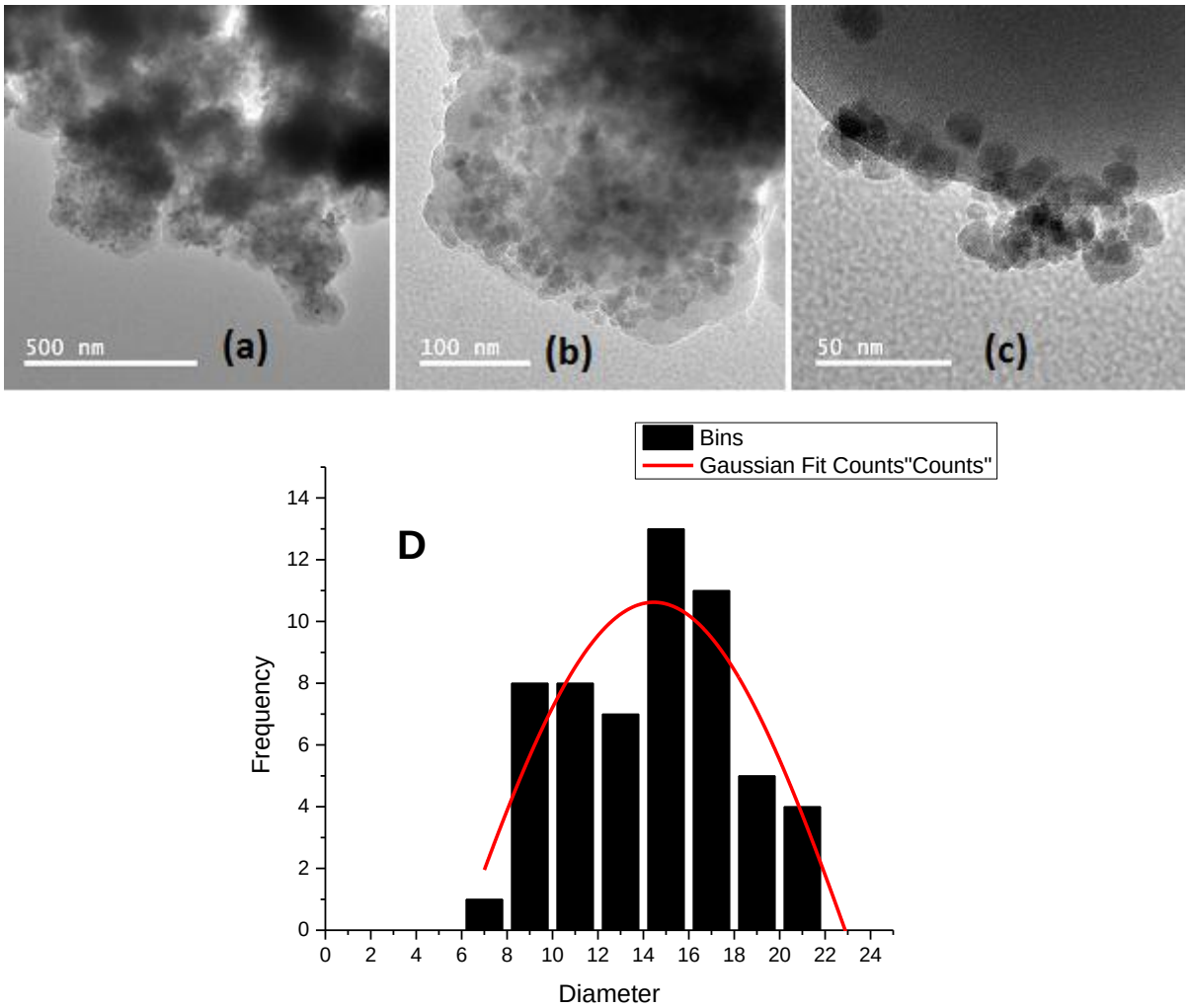

Figure 0-6: TEM images of (a) 500 nm, (b) 100 nm, and (c) 50 nm magnification of Fe_3O_4@SiO_2-MPS and (d) size distribution histogram.

Source: Own authorship

Figure 4.5 (a, b, and c) offers the image of Fe_3O_4@SiO_2-C=C, in which is possible to observe clusters with uniform surface. Evaluating the size distribution histogram of Fe_3O_4@SiO_2-C=C in Figure 4.5d, was found that the adjustment of the Log Normal Equation, and thus determine the value of the d_{med} of Fe_3O_4@SiO_2-C=C which was 14.5 nm (± 0.6), this small increase observed is matches the incorporation of vinyl-groups on the surface of Fe_3O_4@SiO_2.

Table 7 below explains the increase in size of magnetic nanoparticles with the successive modification as a result of silicon shell forming around the magnetic core Fe_3O_4. Surface polymerization of these modified nanoparticles results further increased size in MMIP.

Table 7: Size distribution of Magnetic Nanoparticles

Item type	**Size in Diameter $d_{med\ nm}$**
Fe_3O_4	7.7 (± 0.1)
$Fe_3O_4@SiO_2$	11.3 (± 0.2)
$Fe_3O_4@SiO_2MPS$	14.5 (± 0.6)

Source: Own authorship

The images of TEM-MMIP and TEM-MNIP are presented in Figure 4.6.

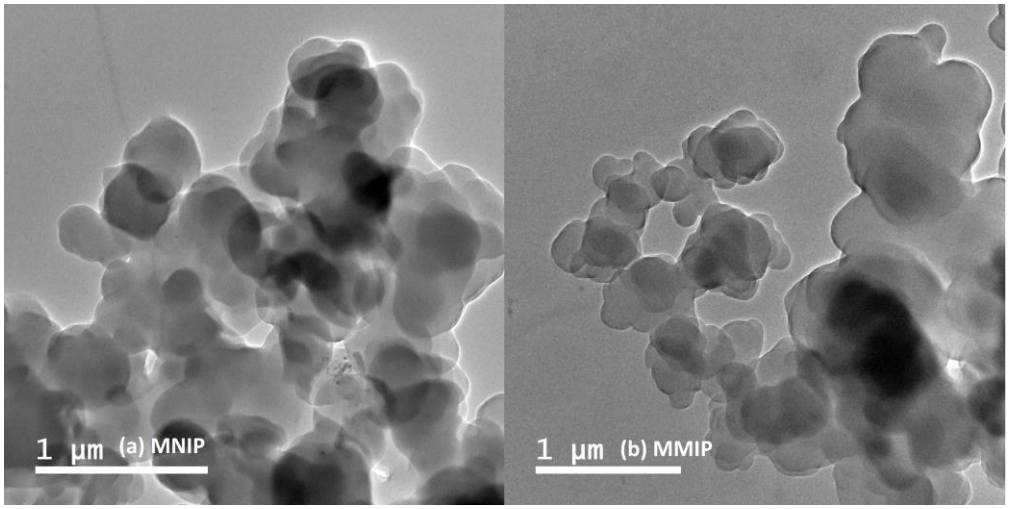

Figure 0-7: TEM images of 1 µm magnification of (a) MNIP, and (b) of MMIP.

Source: Own authorship

By means of Figures 4.6 (a, b, c, and d) one can observe that the MMIP and MNIP respectively, showed similar morphologies arranged in the form of spherical particles, showed

the formation of clusters initially because of the magnetic characteristics of the core, and secondly due to surface polymerization nanoparticles are incorporated very closed to each other. Image tuning could not be conducted for these materials. Visually one can conclude that there is a uniformity in size magnetic polymer particles synthesized on the magnetic nanoparticles of iron oxide, so the core-shell developed in this work has characteristics of advance magnetic imprinted nanomaterials.

4.2.3 Vibrating sample magnetometry (VSM)

The magnetic properties of nanoparticles of Fe_3O_4 is defined by size, surface area and crystal structure. Therefore, the magnetometry is a method used to determine the magnetism of a material when is subjected to a magnetic field.

Based on the response to the presence of an external magnetic field, there are three main classifications for materials: diamagnetic, paramagnetic and ferromagnetic (this last classification there is antiferromagnetic and subclasses ferromagnetic). The nanoparticles of ferromagnetic materials exhibit superparamagnetic characteristics.[83]

Once the nanoparticles used in this work are magnetite, it is expected a behavior of a superparamagnetic material (the nanoparticles, due to their size, have a single domain - that is, a single magnetic orientation; thus presenting superparamagnetism).[54] Therefore, all syntheses were characterized in order to verify, there is conservation of magnetic properties after several modifications. For analysis of the results, the experimental curves were compared with those reported in the literature. The Figure 4.7 shows magnetization curves (M), when applied a magnetic field (H) device.

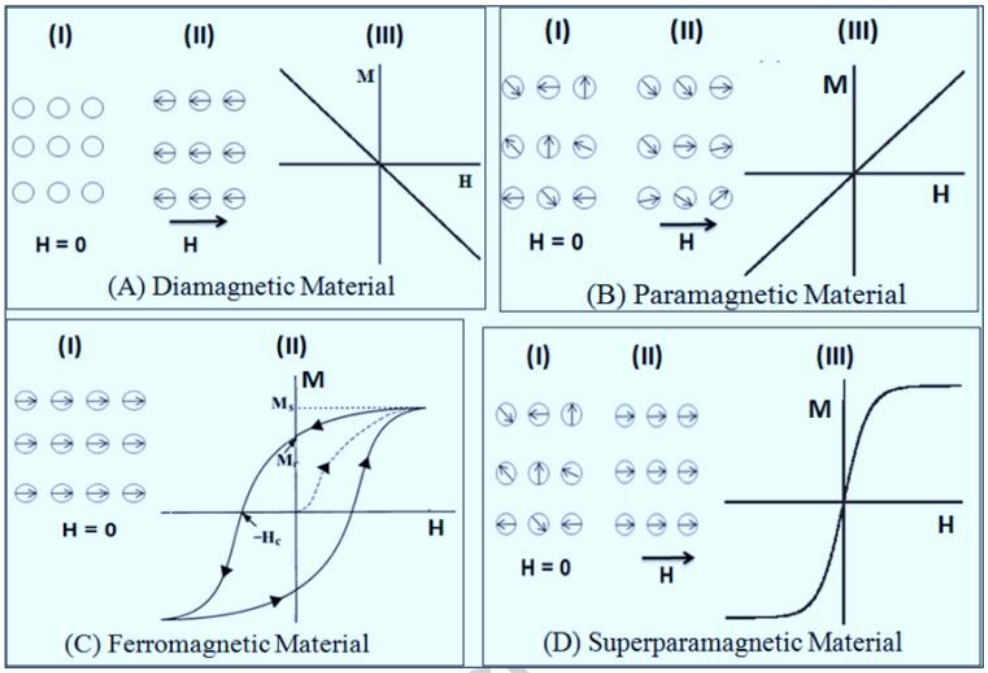

Figure 0-8: Illustration of the magnetic moment (M) of different types of materials under application a magnetic field (H).

Source: SODIPO et al.[83]

For ferromagnetic materials, the material is placed under application a field until it reaches a magnetization of saturation (Ms); generated by the alignment of the magnetic moments of the material. With the decrease of the field, magnetization decreases to the value of remnant magnetization (M_R). The field necessary to remove the magnetization of a material after being subjected to external magnetic field is called the coercive field (Hc) that increases continuously until an opposite value for the saturation magnetization, completing the cycle which is the hysteresis of the material. By varying the orientation of the applied field is removed the magnetization of the material. For materials superparamagnetic due to monodomes, presents a curve of hysteresis of magnetization with high saturation and remanence equal to zero.[83]

For Figures 4.8 to 4.10 one can observe that for three stages of nanoparticles modifications to MMIP and MNIP is observed no hysteresis, no remnant magnetization and neither coercivity (the middle point of the graphs is zero), as expected for superparamagnetic materials.

However, you can view in Figure 4.8 decreasing in magnetization values saturation. For example, for Fe_3O_4 have a value of approximately 65.0 emu g^{-1}, that decreased with modification

with TEOS and then MPS down to 20.0 emu g^{-1}. This can be explained by addition of these reagents on surface of magnetite.

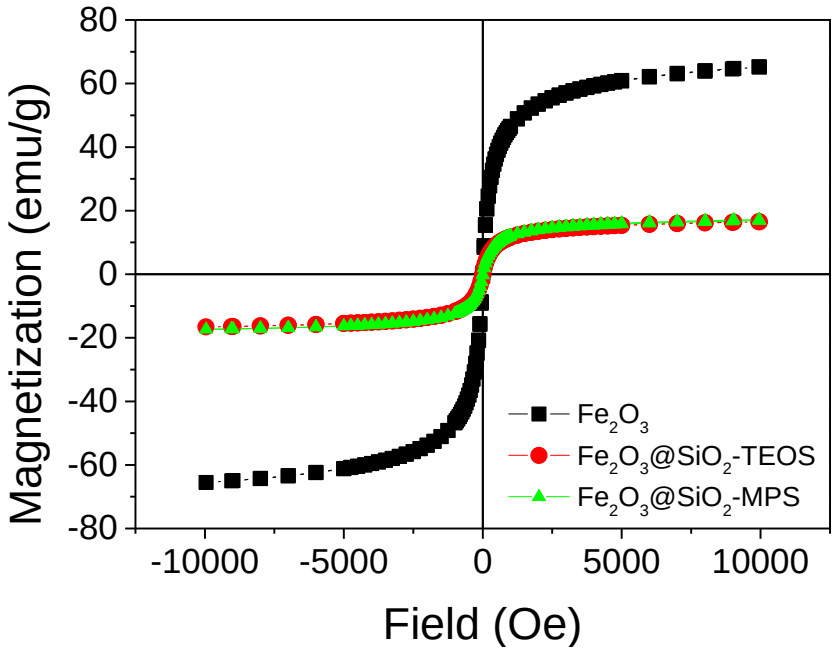

Figure 0-9: The magnetization curves of Fe_3O_4, Fe_3O_4@SiO_2, Fe_3O_4@SiO_2-MPS obtained in this work.

Source: Own authorship

With the addition of functional monomer (FM) and cross-linker, as there is a full covering of MMIP (Figure 4.9), MNIP (Figure 4.10) surfaces, the magnetization value further decreased until 0.6 and 1.5 emu g^{-1}, respectively.

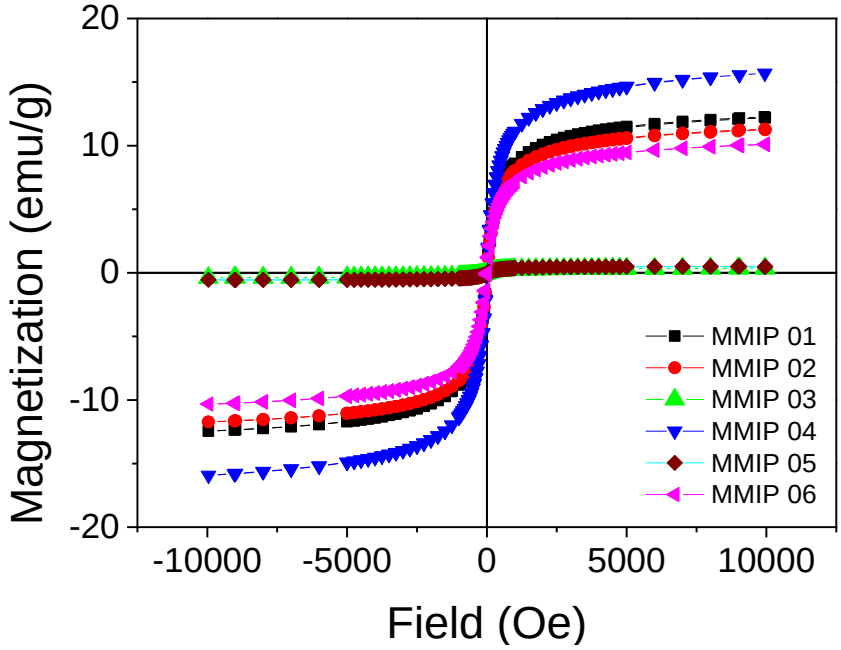

Figure 0-10: The magnetization curves of Fe_3O_4@MIP of polymers.
Source: Own authorship

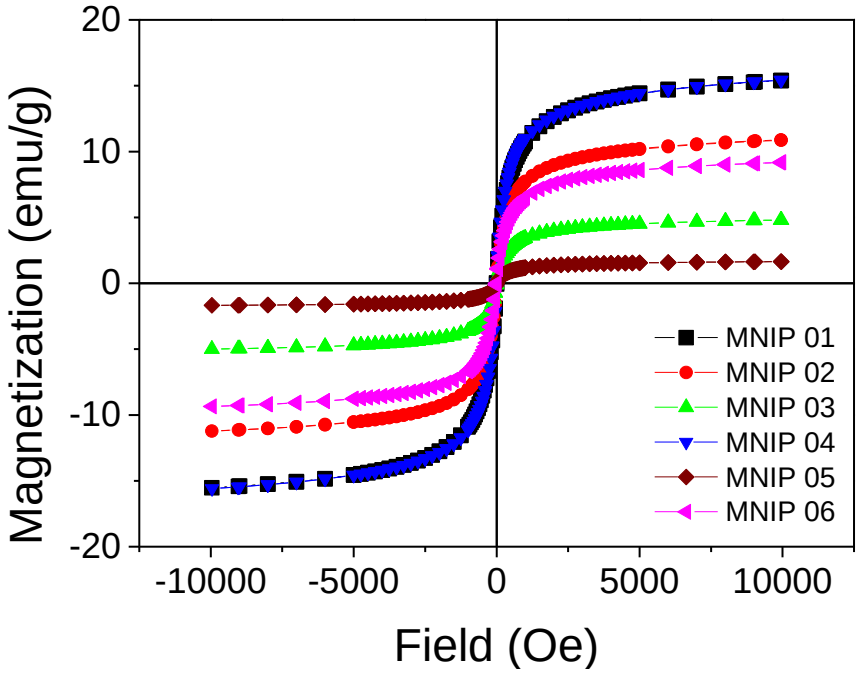

Figure 0-11: The magnetization curves of Fe_3O_4@NIP of polymers..
Source: Own authorship

These results are in consonance with experimental observations, in that the application of field magnetic from a neodymium magnet was much less efficient in separating polymer the solution than the magnetite nanoparticles; since the large amount of material coating the nanoparticles decreased their magnetic response.

4.2.4 UV-vis behavior

To determine the wavelength at which the Caffeine exhibits maximum absorbance, absorption spectra were performed in the range of 200 to 400 nm. The profile of the absorbance spectra in the UV-vis region of the Caffeine (Figure 4.12) is observed a maximum molar absorbance at 278 nm in methanol. In Figure 4.13 showed the corresponding calibration curve.

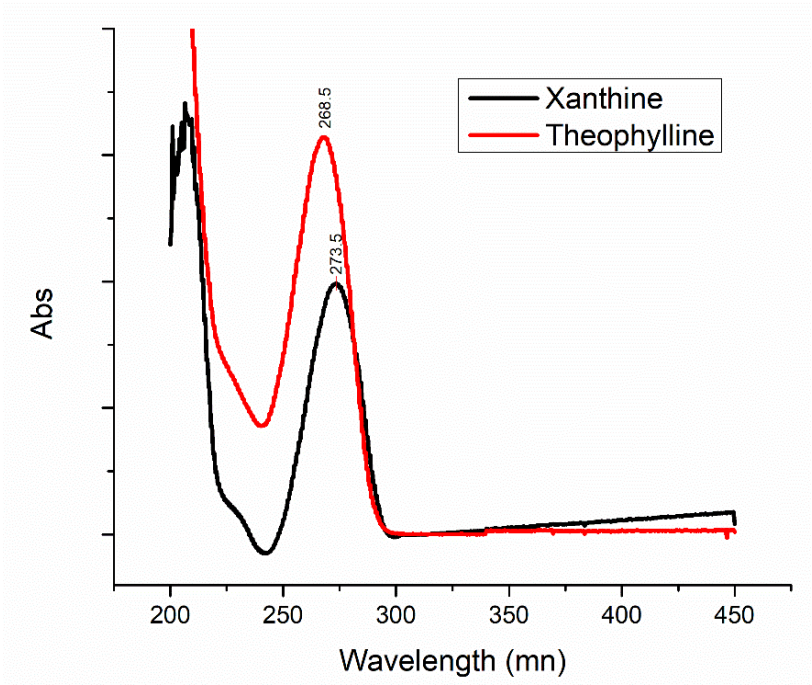

Figure 0-12: Absorption spectrum in the UV-Vis region for different concentrations of Theophylline and Xanthene soluble in water and dilute NaOH (aqueous) respectively.

Source: Own authorship

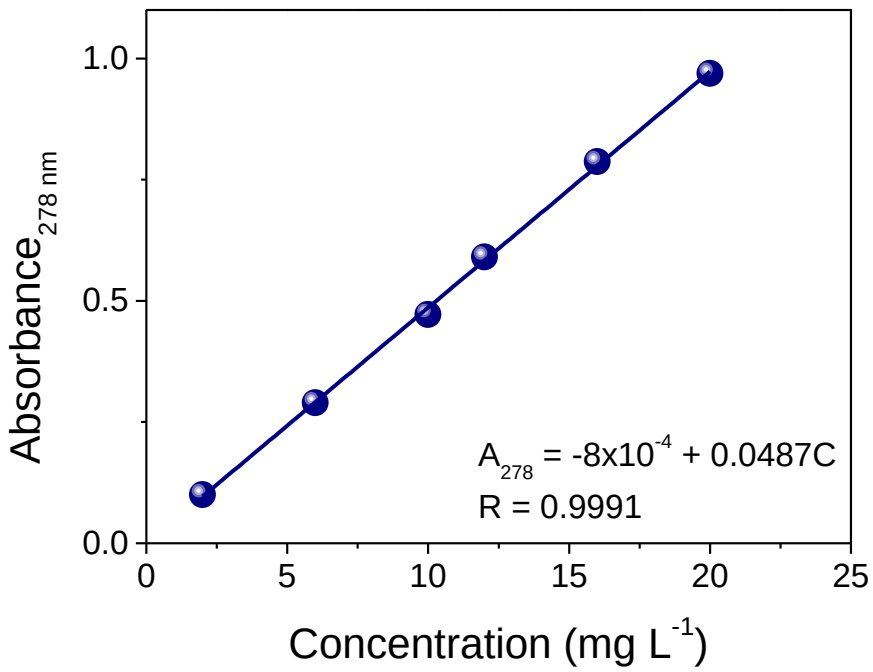

Figure 0-13: Analytical curve referring to the maximum absorbance at wavelength 278 nm, used like solvent methanol.

Source: Own authorship

The caffeine has one band of high intensity at 287 nm that is in the ultraviolet region, which is attributed to the unsaturation of the aromatic ring corresponding to the electronic transitions of its double conjugated bonds. It should be noted that above 40 mg L^{-1}, the absorbance reached values higher than 1. Thus, to avoid deviations in Beer's law, it is recommended to work up to 20 mg L^{-1}. In addition, caffeine has high absorptivity coefficient, since small amounts will allow high absorption.

For selectivity studies analytical curves of two molecules with very close chemical structure of analyte caffeine, such as theophylline and xanthine also were plotted, in Figures 4.14(b) and (c). In addition, a new analytical curve of caffeine prepared in water solvent is present in 4.14(a). The difference of solvents (Figure 4.12 and 4.13) was necessary because the first data was used to monitor the washing step of the MMIP and MNIP in methanol, and the second solvent water is used in the adsorption and selectivity experiments.

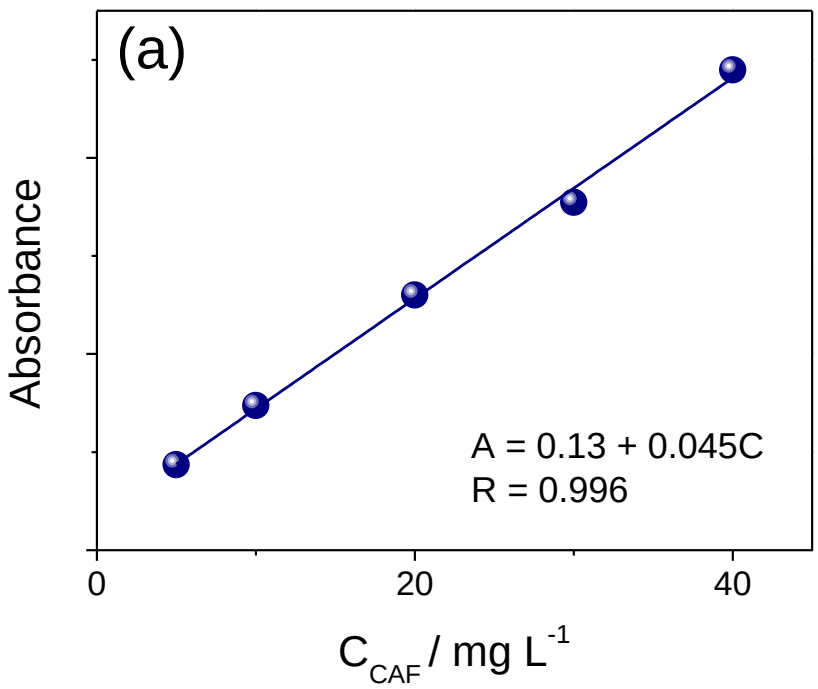
(a)
Absorbance
A = 0.13 + 0.045C
R = 0.996
0
20
40
C_CAF / mg L^-1

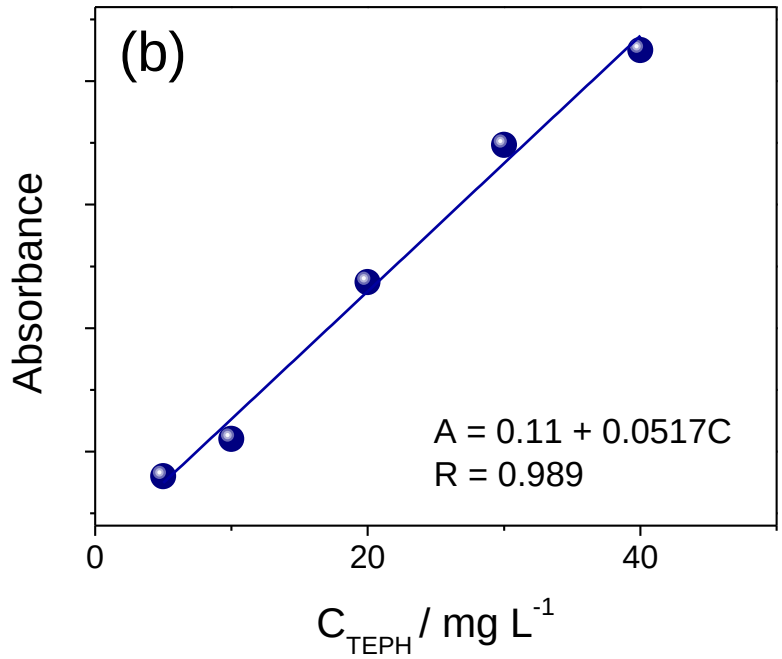
(b)
Absorbance
A = 0.11 + 0.0517C
R = 0.989
0
20
40
C_TEPH / mg L^-1

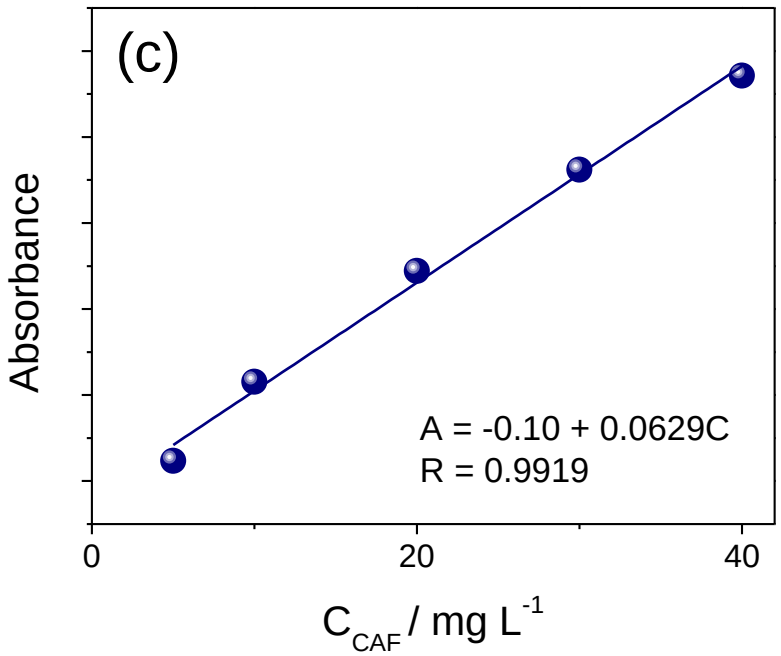

Figure 0-14: Calibration curve for caffeine - CAF (a), theophylline - TEPH (b) prepared in deionized water and (c) xanthine - XAN in 0.01 mol L^{-1} NaOH solution.
Source: Own authorship

4.3 CHROMATOGRAPHIC METHOD

In order to assess the adsorption efficiency of different polymers (MMIP) synthesized was used high-performance liquid chromatography coupled with UV-vis detector, the chromatograms are presented in Figure 4.14 which were used to plot the analytical curve observed in Figure 4.15.

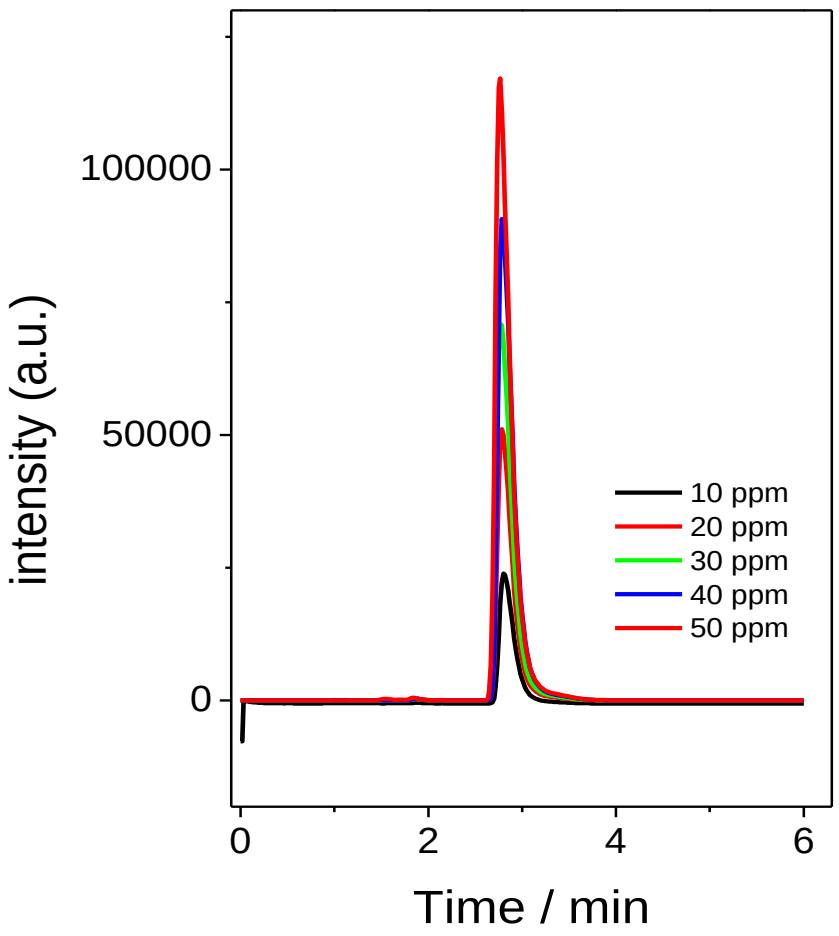

Figure 0-15: Chromatograms obtained for Caffeine, under 3.3. procedure.
Source: Own authorship

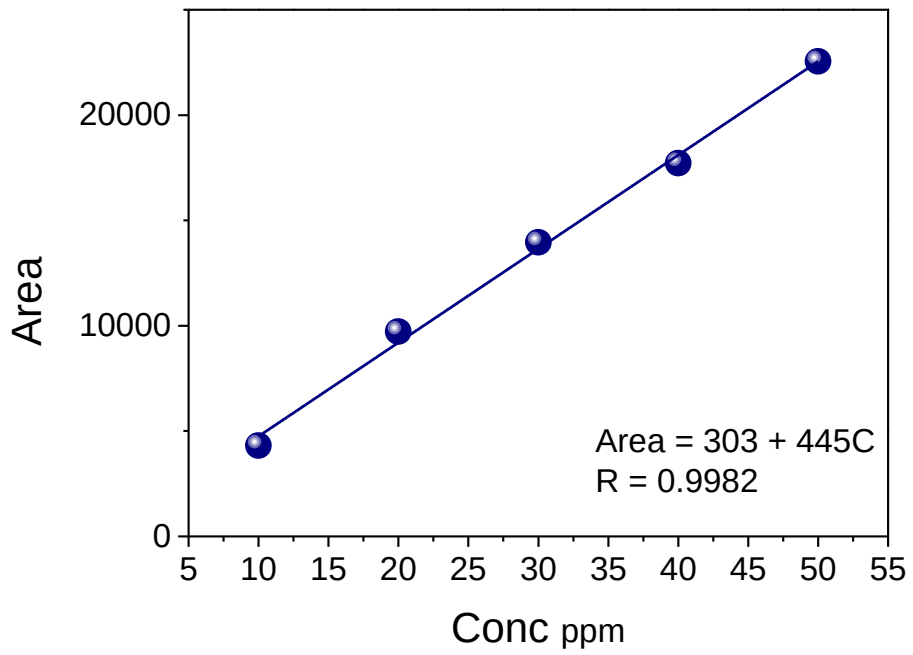

Figure 0-16: Analytical curve for caffeine obtained in HPLC/UV-Vis, in conditions previously described in 3.3. section.

Source: Own authorship

HPLC method employed exhibits better qualitative and quantitative results for caffeine at retention time of around 2.6 min, with a linear response between 10 to 50 ppm (r^2 0.997), which was used in the further experiments. Application of MMIP for analysis in real sample requires a better separation technique for analyte (caffeine) from complex matrix for this purpose HPLC is the best option.

4.4 REMOVAL OF THE CAFFEINE MOLECULE FROM THE MIP STRUCTURE

Different MMIP and MNIP have synthesized, after MIP synthesis an initial step is purification of MMIP and MNIP which is achieved by magnetic separation in bulk solvent. As shown in figure 4.17 water was normally used, after several washing cycles of the polymer became visibly free from all residues of the reaction mixture. Second major step is bulk washing using Buchner funnel equipped with a suction pump, here MMIP and MNIP are transferred to filter paper fitted on the filtration assembly, turning on the pump and genteelly pouring solvent over polymer in Buchner funnel, further purify polymer produced. Third important step is the removal of template molecule from the cavities of the imprinted polymer in a way that the entry of the analyte of interest into the cavity of the imprinted polymer is feasible, allowing the reconnection in a subsequent analysis. For this reason, the removal of caffeine from the MMIP was monitored by means of spectrophotometric measurements. For this, the first washing solution was a mixture of acetic acid (5 mL) added to 100 mL of methanol and the second was methanol in a Soxhlet system in order to remove the analyte from the initially six types of polymers synthesized.

For seventh type of MMIP and MNIP, deionized water and acetonitrile are also used. Washing solutions were changed and monitored after every 8 hours by UV-Vis spectrophotometry, as shown below in Figure 4.17 detail describes the above procedures.

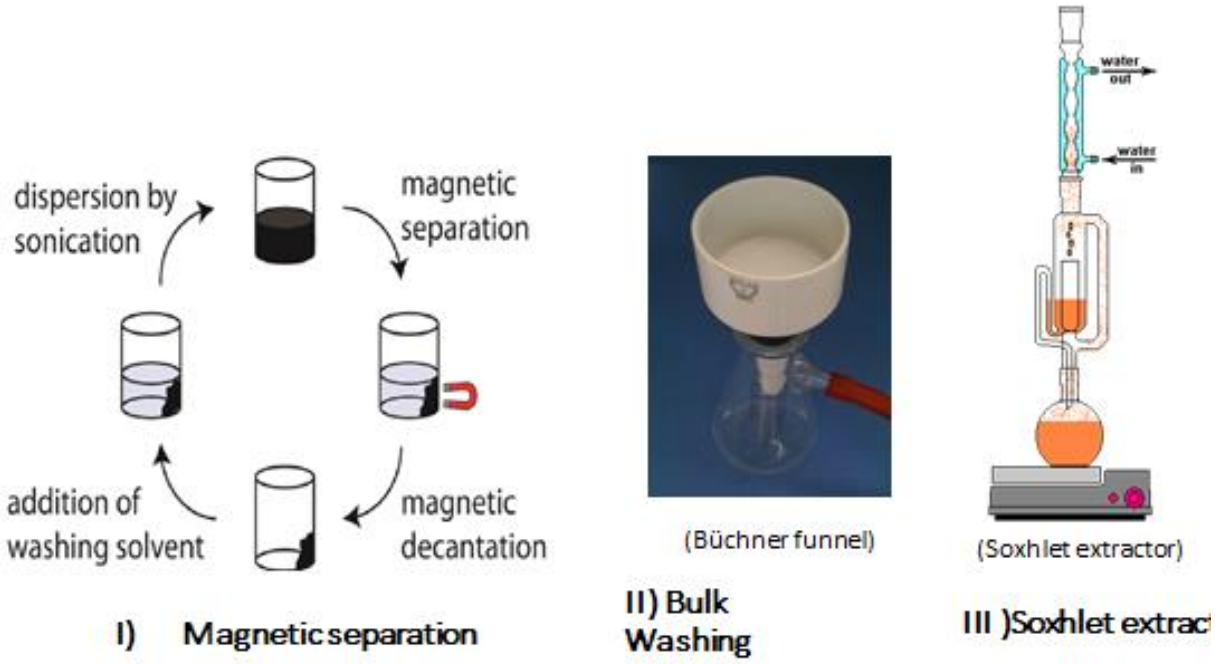

Figure 0-17: Purification Washing procedure. I) Magnetic separation, II) Bulk Washing, III) Soxhlet extractor.

Source: Own authorship

4.5 MMIP OPTIMIZATION EXPERIMENTS

In order to maximize the retention of caffeine to MMIP, evaluation of the adsorption solvent, mass dosing and interaction time to achieve the equilibrium were carried out. At all stages, the quantification of analyte was evaluated by UV-vis spectrophotometry

The first study was the adsorption solvent in which the caffeine must be enough solubilized and the same time can be interacting with the polymer, whereby the medium in which the analyte is solvated directly affects its connection to the polymer cavities. Caffeine was solubilized in methanol, ethanol, water and different ratios between these solvents. Of the various types of solution evaluated initially methanol was used because high solubility of caffeine. However, this solvent was latterly replaced by water, that shown to be best in binding results being the solvent adopted for the further studies.

The next experiment was the optimization of the polymer mass to recognition of caffeine. For this, were evaluated between 0.5 to 25.0 mg mL^{-1} of polymer for the initial six types of MMPs Table 5, but no satisfactory results were obtained, using these quantities with all those materials synthesized. Most probably due the types of functional monomer used exhibit low interactions with analyte (caffeine) and secondly the is the ratio between template, functional monomer and cross- linker were 1:4:10 respectively, which were then changed to 1:8:20 for the next synthesis.

Thus, in a next experiment was evaluated the MMIP 07 using two mass corresponding to 10 and 1 mg mL^{-1} of each polymer. Concomitantly, was studied the time for the best interaction between the polymer and the analyte. To do this, initially was set up a mass of 10 mg mL^{-1} MMIP, where there was only a slight difference between MMIP and MNIP, as varied the interaction time Figure 4.18.

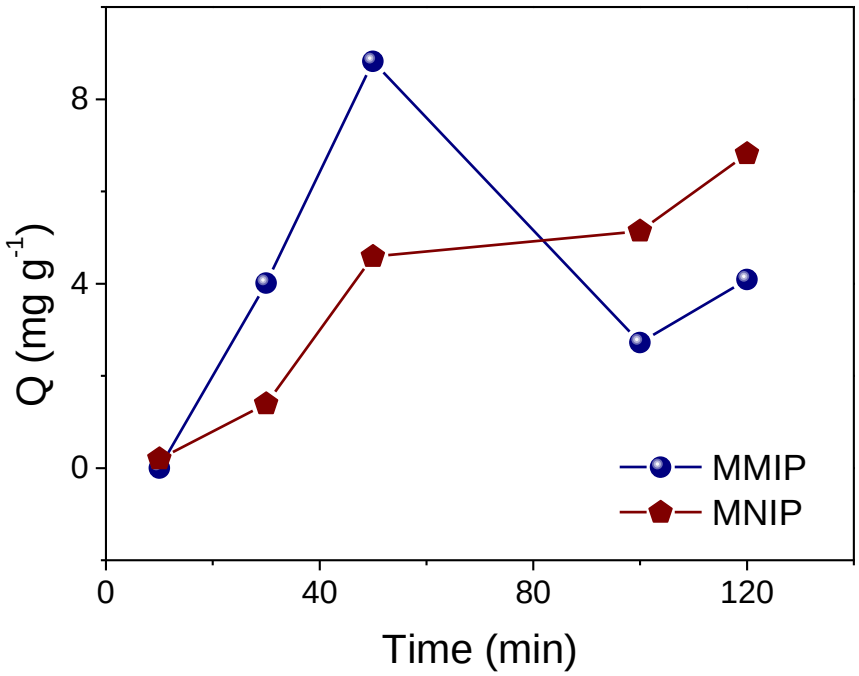

Figure 0-18: Results for optimizing the interaction time (analyzed range 10 to 120 Minutes) between MMIP (10 mg mL^{-1}), caffeine (20.0 mg L^{-1}) prepared in methanol.

Source: Own authorship

Then, since the results showed in Figure 4.18, were not satisfactory, the polymer amount was reduced to 1 mg mL^{-1} and the results are showed in Figure 4.19.

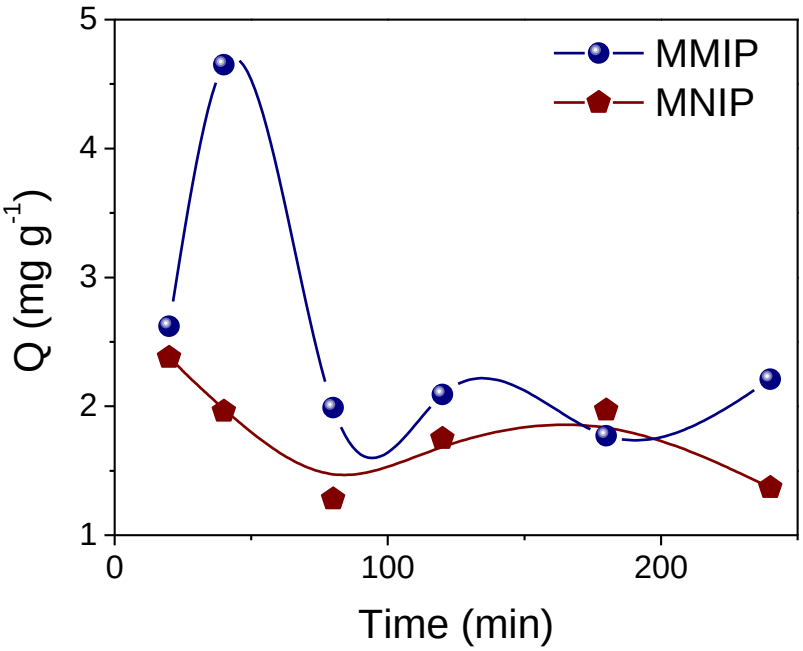

Figure 0-19: Results for optimizing the interaction time (analyzed range 20 to 240 minutes) for 1 mgL^{-1} polymer of 20.0 mg L^{-1} caffeine prepared in water.
Source: Own authorship

Figure 4.19, are showed the results obtained a reduced amount of polymer 2 mg in 2 mL (1.0 mg mL^{-1}). In this case is possible to observe the better interaction time occurs at 40 min, in which, there is a higher values of adsorption capacities as well as difference between the retention percentage of caffeine for MMIP and MNIP. Thus, was this time set to further experiments.

Finally, MMIP and MNIP were evaluated in solutions with different pH values (Figure 4.20. It is possible analyze that around pH 7.0 – 8.0 the MMIP and MNIP adsorption is similar. However, to pH between 3 – 5 and 9.0 – 10.0 the difference between MMIP and MNIP is more evident. Thus, in order to follow with further experiments, in this work was set up the solution with pH 9.0.

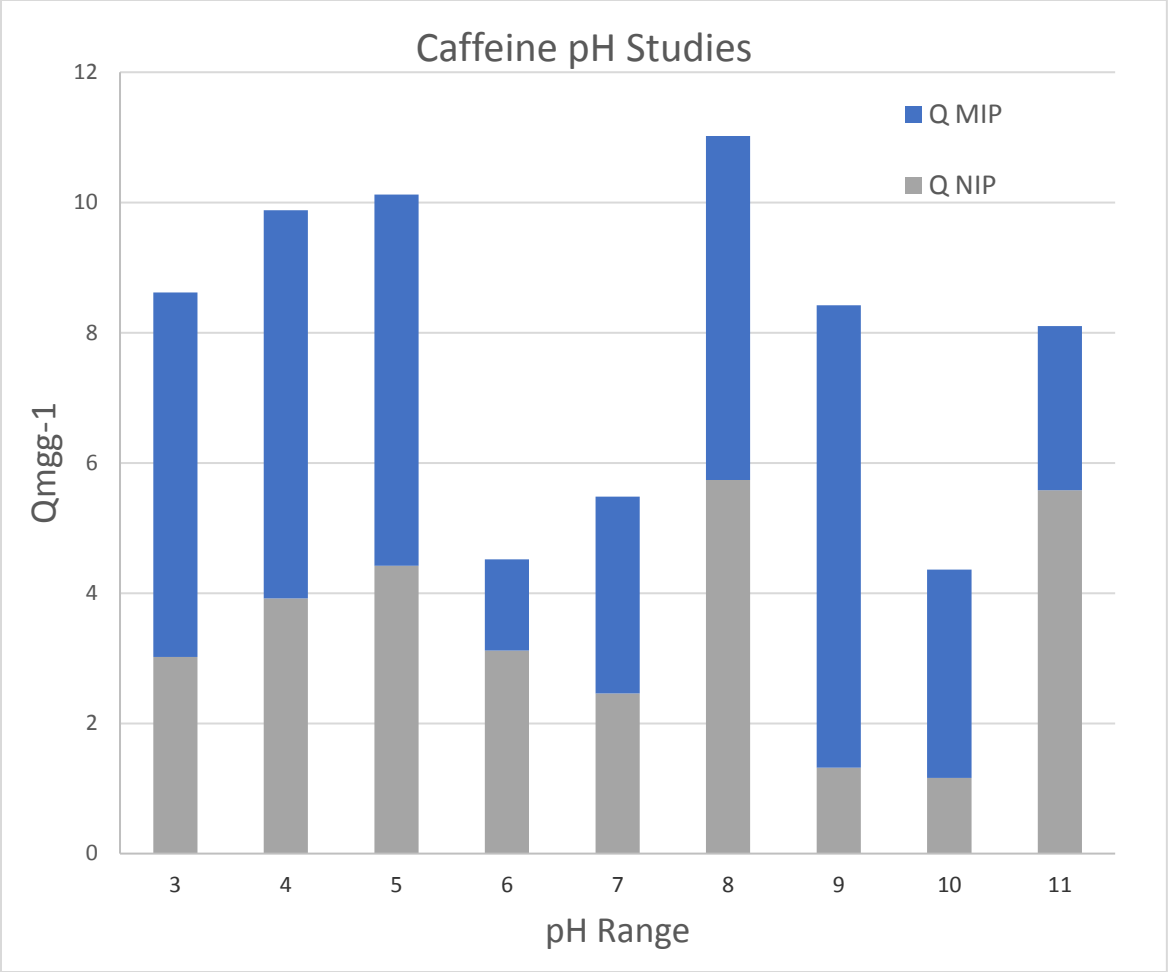

Figure 0-20: 20 mg L^{-1} Caffeine adsorption profile as function of pH in the range from 3.0 to 11.0 to 0.5 mg mL^{-1} MMIP and MNIP at interaction time to 40 min.
Source: Own authorship

Once optimized these parameters, the next experiment was carried out in order to construct the adsorption isotherm.

4.6 ADSORPTION ISOTHERM, SELECTIVITY AND AFFINITY CONSTANTS (K_A)

The adsorption isotherm constructed using the parameters previously optimized for MMIP and its comparison with interfering compounds having similar molecular structures

theophylline (THP) and xanthine (XNT) was carried out. The Figure 4.21 shows the differences obtained in adsorption of caffeine for the evaluated materials.

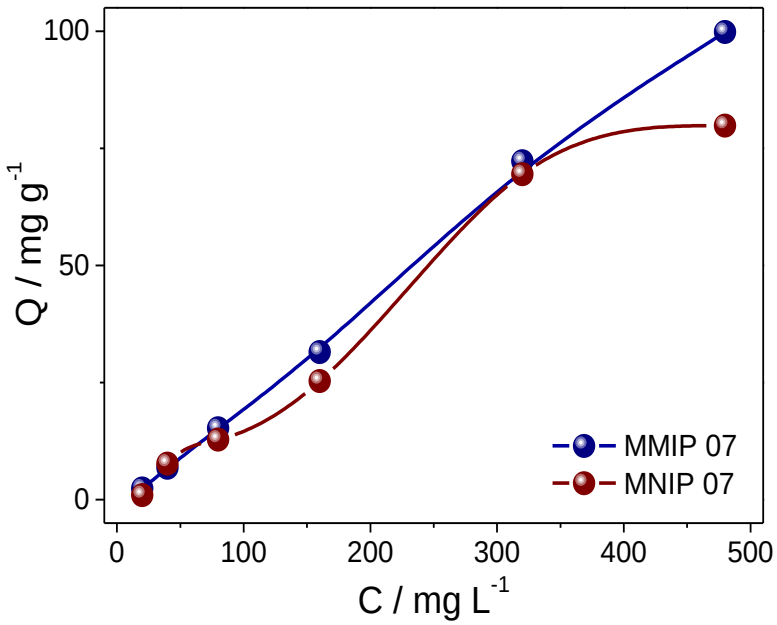

Figure 0-21: Caffeine adsorption isotherm (in the concentration range of 20 to 480 mg L^{-1}) to MMIP (or MNIP) at 1.0 mg mL^{-1} of polymer to interact for 40 min and pH 7.0.

Source: Own authorship

Is evident the different on the adsorption profile for the MMIP and MNIP. In MMIP is possible to observe than the adsorption profile is the desired for an isotherm: increased adsorption analyte with increased concentration up to saturation, indicating that all sites are occupied. On the other hand, when analyzed the isotherm obtained for the MNIP, it is possible to observe than this isotherm presents at Type IV profile, indicating from 160 mg L^{-1} a not specific interaction.

Figures 4.22 and 4.23 show the isotherms obtained for theophylline (THP) and xanthine (XTN) with the MMIP and MNIP synthesized for (CAF) Caffeine.

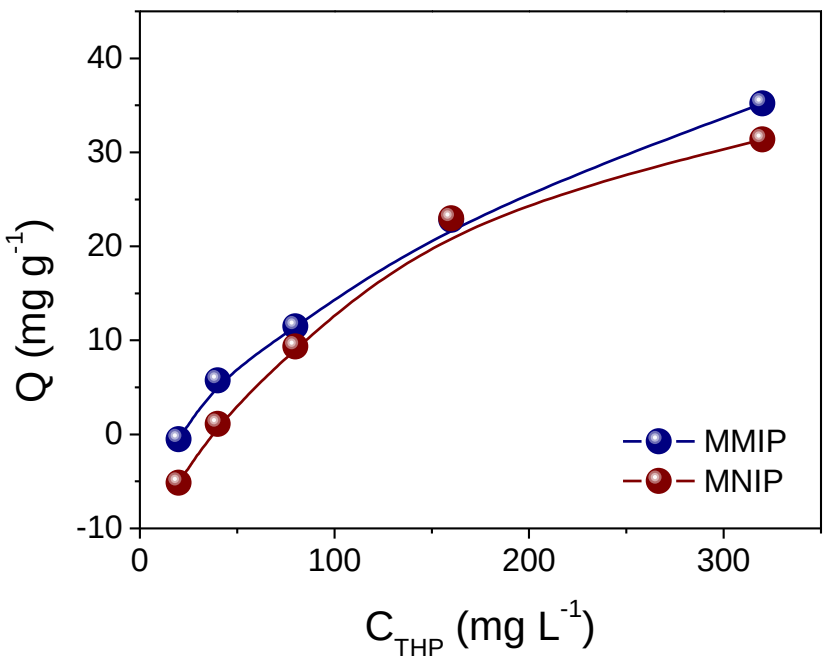

Figure 0-22: Adsorption isotherm for comparison of selectivity (THP-Theophylline).
Source: Own authorship

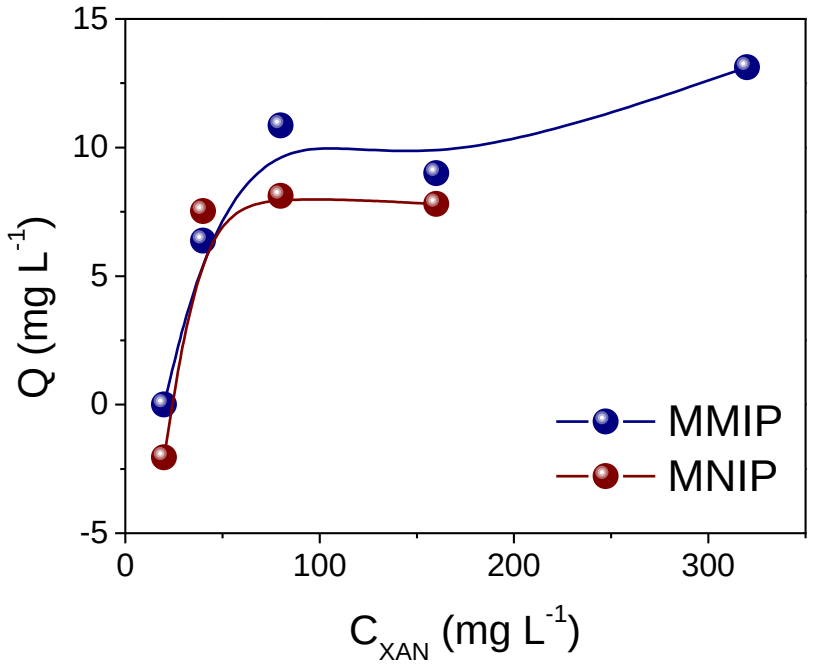

Figure 0-23: Adsorption isotherm for comparison of selectivity (XTN-Xanthine)
Source: Own authorship

Figures 4.24 shows a comparison for the three compounds studied and it is possible to observe with the increasing concentration of the analyte, the caffeine is preferably adsorbed in the selective cavity on the MMIP. These results show that the MMIP for caffeine was much more efficient as expected.

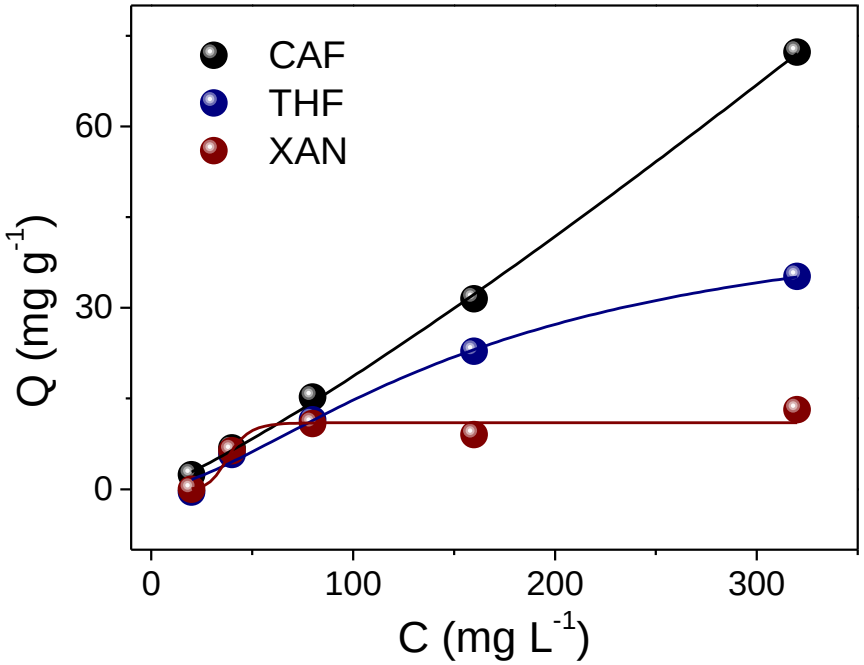

Figure 0-24: Adsorption isotherms for comparison of selectivity (CAF-Caffeine, THP-Theophylline, and XTN-Xanthine until 320 mg L-1 for 1.0 mg mL-1 of materials).

Source: Own authorship

Finally, with isotherms of Figures 4.22 – 4.24 were estimated the affinity constant (Ka) of MMIP and MNIP to three compounds (caffeine, theophylline and xanthine). For the calculation, we used the Langmuir-Freundlich adsorption model.

It is a combined form of the Langmuir and Freundlich expressions deduced to predict heterogeneous adsorption systems and to circumvent the limitation of the increasing adsorbate concentration associated with the exponential expression of the Freundlich isotherm model.[84]

The Langmuir-Freundlich fit is given by the following relationship:

$$Q = \frac{Q_M \times K_L \times C^{\beta}}{1 + K_L \times C^{\beta}} \qquad (Equation\ 5)$$

Where Q_M is the maximum in the adsorption capacity (mg g^{-1}), K_L is the affinity parameter (L mg^{-1}), C is the concentration at equilibrium of the adsorbate (mg L^{-1}) and β is the measure of the adsorption intensity or heterogeneity of the surface and can vary between 0 and 1. The more its value approaches zero it can be concluded that the surface is more heterogeneous.

From the experimentally adjustment $K_{L,}$ is possible to estimate the affinity constant (K_{AF}, express in mol L^{-1}) of caffeine to MMIP or MNIP (Table 6).

In all cases based on correlation coefficient (R^2) the Langmuir-Freundlich model was best fit to the experimental data for these materials. Thus, using the parameters obtained of the each mathematical adjustments, were obtained that the affinity constant for MMIP for caffeine is K_{AF} = 9.6 x 10^2 mol L^{-1} in comparison with theophylline; K_{AF} =6.85x10^{-3} mol L^{-1} and xanthine K_{AF} = 6.4 x 10^1 mol L^{-1}. As expected and reported in the literature[54], imprint affinity constant is higher, since the recognition sites were generated, with exact size and conformation of the analyte. In Table 8 also are showed partition coefficient, selectively coefficient, imprinting factor, and Selectivity factor with relation to the affinity constant (K_{AF}).

Table 8: Binding parameters for MMIP and MNIP for Caffeine in comparison with theophylline and xanthine.

Analyte	**Polymer**	$K_P = \frac{Q}{C}$	$\alpha = \frac{K_P^{Analyte}}{K_P^{Interfering}}$	$I = \left(\frac{K_P^{MIP}}{K_P^{NIP}}\right)_{Anal}$	$S = \frac{I_{Analyte}}{I_{Intefering}}$	**K_{AF} / mol L^{-1}**

Caffeine	MMIP	1.56		1.25		**960**
	MNIP	1.25				9.31
Theophylline	MMIP	1.43	1.4	0.99	1.3	6.8×10^{-3}
	MNIP	1.44	1.3			1.8×10^{-2}
Xanthine	MMIP	0.06	3.6	1.14	1.1	64.2
	MNIP	0.05	3.3			0.57

Source: Own authorship

4.7 Application in beverage samples

After all the synthesis, characterization and evaluation of efficiency of MMIP for caffeine, where carried out adsorption experiments in commercial samples of Black tea, Coffee and soda coke, in order to evaluate the feasibility of application of the developed materials, and the Figure 4.25 shows the sample treatment procedure in this study. First is the boiling stage for tea and coffee, then transferring real sample to solution containing MMIP and MNIP, details of sample were given in table 6 of section 3.5.9. These sample tubes previously labeled are setup on the homogenizer, and interacted for a given time period. After completion of time duration sample tubes are arranged on a rack according to their identified. One by one Magnetic polymers (MMIP / MNIP) were settled down rapidly by the external magnet, taking out the clear solution in a disposable crying for passing through 0.2µm filter. The filter samples then analyzed by UV-Vis and HPLC.

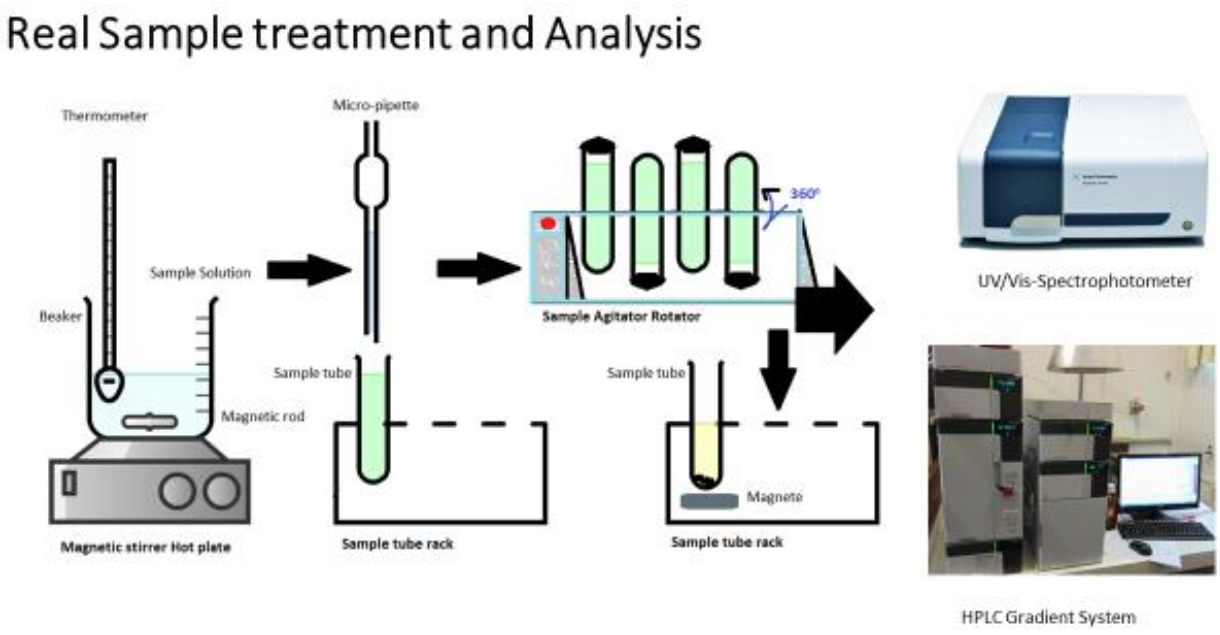

Figure 0-25: Real sample treatment analysis.
Source: Own authorship

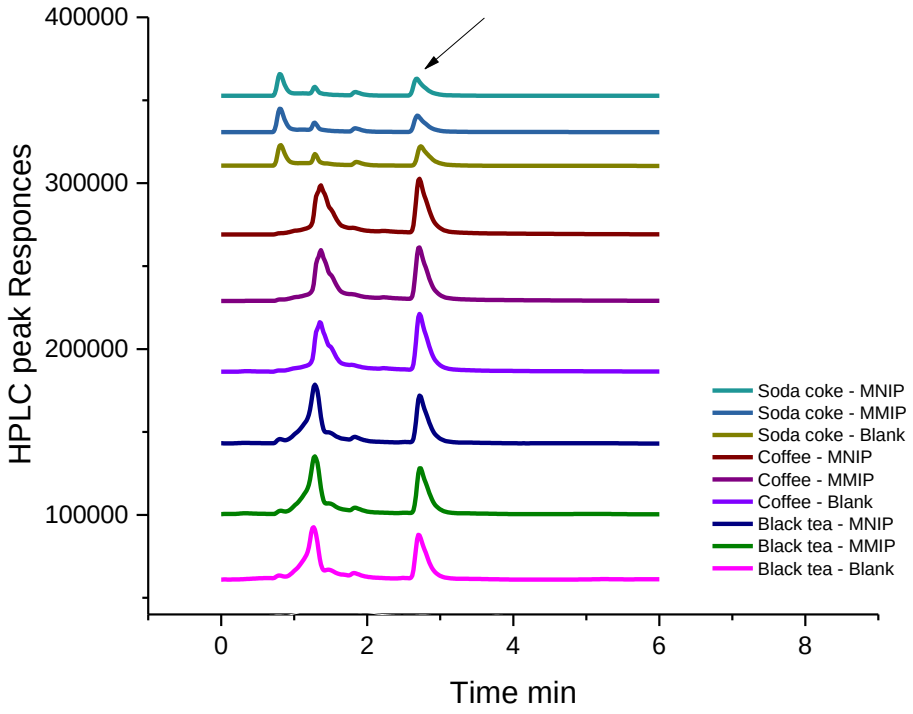

Figure 0-26: Chromatograms obtained in the analysis of samples.
Source: Own authorship

The central objective of this procedure was determined if the imprinted synthesized polymers can be used in a real situation of laboratory or quality control sector. However, despite the many efforts made, this was not possible in this stage, as shown in figure4.26. Since percentage values of adsorption for MMIP and MNIP were close and low, such as are indicating in Table 8.

This result, indicating that the imprinted polymer developed did not show good performance in the sample analysis. The fact that it did not achieve a favorable result in the application of the MMIP synthesized does not invalidate its efficiency since it was previously proven in the studies of optimization, characterization and selectivity. Thus, more in-depth studies for pretreatment of the sample, as well as variables such as adjustment of pH of sample solution, among others parameters should still be performed.

Table 9: Recovery values obtained in the beverage food analysis compared with the Blank values.

Sample	**Recovery value of the caffeine (%) used like reference the Blank concentration (caffeine in sample)**	
	In MMIP	**In MNIP**
Black Tea	3.3 %	0 %
Coffee	6.4 %	3.2 %
Soda coke	16.4 %	16.4 %

Source: Own authorship

The experiments carried out allowed a learning in the treatment of samples containing caffeine, which will be used in later experiments in order to evaluate other types of samples.

In Table 9, is showed the calculated value of caffeine in each sample evaluated after adsorption experiments and the corresponding amount in each sample.

Table 10: Concentration in ppm of the caffeine in the solution after adsorption experiments and the samples, which were evaluated and estimated by HPLC method.

Sample	Caffeine concentration (ppm) in solution		
	MIP	**NIP**	**Blank**
Black Tea	14.6	15.1	15.1
Coffee	17.7	18.3	18.9
Soda coke	4.6	4.6	5.5

Source: Own authorship

It is important emphasize than in all cases a slightly better efficiency can be observed for the MMIP compared to their corresponding MNIP, since adsorbed the analyte in a higher amount.

5 Conclusions - Perspectives

In this thesis we demonstrated, the great potential of molecularly imprinted polymers as selective receptors in “real world” applications. The main challenge was to design a MIP that could efficiently capture the target molecules in an extremely complex and unfavorable environment. Secondly MMIP could be easily separated from the complex medium after interaction by its super paramegnatic nature. Here demonstrated a systematic study in order to synthesize various magnetic selective materials to caffeine.

Our first attempts, where the MIP was prepared acrylonitrile (ACN) and EGDMA were not much successful, as very small or even no binding was. Also, polymers synthesized used the structural monomer TRIM similarly provided unsatisfactory results. The polymer synthesized with MAA in the proportion 1:4:10 (template: monomer: cross-linker) shown very low binding as compared to higher proportion (1:8:20) respectively.

The porogenic solvent, also was essential to obtain the best MMIP polymer. In this sense, acetonitrile provided a MMIP with superior properties than those synthesized used ethanol.

The non-covalent MMIP, synthetized with MMA in acetonitrile in a 1:8:20 ratio presenting specific selective adsorption capacities for caffeine with respect to theophylline and xanthine, the affinity constant presented was greater for the MMIP, showed than the MMIP synthesized was highly selective, since both molecules have very similar chemical structures.
In application of the MMIP synthesized more studies should be carried out to achieve satisfactory results. Since, as the group experience the unsatisfactory results are due to the inadequate treatment to samples, and not due to the MMIP synthesized.

This PhD thesis has allowed us to better understand the significant advantages of MIPs as tailor-made synthetic receptors, with emphasis on recognition in complex environments. The field of molecular imprinting has been developed remarkably since the pioneering studies of Wulff and Mosbach, owing to the intensive research performed in the recent years. Extensive efforts towards the optimization of synthetic protocols and the rational design of MIPs have allowed to circumvent some of the issues related to MIP synthesis such as low affinity and selectivity in complex environments as well as the successful targeting of biomacromolecules.

Hence, it is evident that MIPs can be more than an alternative to antibodies, being more versatile, robust and cost-effective. Nowadays, MIPs feature outstanding recognition

6 References

1. Nehlig, A., Daval, J. L. & Debry, G. Caffeine and the central nervous system: mechanisms of action, biochemical, metabolic and psychostimulant effects. *Brain Res. Brain Res. Rev.* **17**, 139–70 (1992).
2. Kliszczewicz, B. *et al.* The influence of citrus aurantium and caffeine complex versus placebo on the cardiac autonomic response: a double blind crossover design. *J. Int. Soc. Sports Nutr.* **15**, 34 (2018).
3. Mitchell, D. C., Knight, C. A., Hockenberry, J., Teplansky, R. & Hartman, T. J. Beverage caffeine intakes in the U.S. *Food Chem. Toxicol.* **63**, 136–142 (2014).
4. Weinberg, B. A. & Bealer, B. K. *The world of caffeine : the science and culture of the world's most popular drug*. (Routledge, 2001).
5. Meyers, H. *"Suave Molecules of Mocha" – Coffee, Chemistry, and Civilization*. (2005).
6. Somogyi, L. P. *Caffeine Intake by the U.S. Population*. (2010).
7. Nathanson, J. A. Caffeine and related methylxanthines: possible naturally occurring pesticides. *Science* **226**, 184–7 (1984).
8. Foelix, R. F. *Biology of spiders*. (Oxford University Press, 2011).
9. Hollingsworth, R. G., Armstrong, J. W. & Campbell, E. Caffeine as a repellent for slugs and snails. *Nature* **417**, 915–6 (2002).
10. Sin, H., Radford, A., Witmer, G. W. & Pitt, W. C. COQUI FROG RESEARCH AND MANAGEMENT EFFORTS IN HAWAII COQUI FROG RESEARCH AND MANAGEMENT EFFORTS IN HAWAI'I. (2007).
11. Gartrell, B. & Reid, C. Death by chocolate: A fatal problem for an inquisitive wild parrot. *N. Z. Vet. J.* **55**, 149–151 (2007).
12. Tawde, S. N., Puschner, B., Albin, T., Stump, S. & Poppenga, R. H. Death by Caffeine: Presumptive Malicious Poisoning of a Dog by Incorporation in Ground Meat. *J. Med. Toxicol.* **8**, 436–440 (2012).
13. Witt, P. N. & Rovner, J. S. *Spider communication : mechanisms and ecological significance*. (Princeton University Press, 1982).

14. Brittain, H. G. *Profiles of drug substances, excipients, and related methodology. Volume 33*. (Elsevier/Academic Press, 2007).
15. Klosterman, L. *The facts about caffeine*. (Marshall Cavendish Benchmark, 2006).
16. Bower, R. S., Anderson, A. D. & Titus, R. W. Determination of Caffeine. *Anal. Chem.* **22**, 1056–1058 (1950).
17. Nehlig, A., Daval, J. L. & Debry, G. Caffeine and the central nervous system: mechanisms of action, biochemical, metabolic and psychostimulant effects. *Brain Res. Brain Res. Rev.* **17**, 139–70 (1992).
18. Warren, G. L., Park, N. D., Maresca, R. D., McKibans, K. I. & Millard-Stafford, M. L. Effect of caffeine ingestion on muscular strength and endurance: a meta-analysis. *Med. Sci. Sports Exerc.* **42**, 1375–87 (2010).
19. Fisone, G., Borgkvist, A. & Usiello, A. Caffeine as a psychomotor stimulant: mechanism of action. *Cell. Mol. Life Sci.* **61**, 857–72 (2004).
20. Ferré, S. An update on the mechanisms of the psychostimulant effects of caffeine. *J. Neurochem.* **105**, 1067–79 (2008).
21. Ferré, S. *et al.* Allosteric mechanisms within the adenosine A2A-dopamine D2 receptor heterotetramer. *Neuropharmacology* **104**, 154–60 (2016).
22. Liguori, A., Hughes, J. R. & Grass, J. A. Absorption and subjective effects of caffeine from coffee, cola and capsules. *Pharmacol. Biochem. Behav.* **58**, 721–6 (1997).
23. Blanchard, J. & Sawers, S. J. A. The absolute bioavailability of caffeine in man. *Eur. J. Clin. Pharmacol.* **24**, 93–98 (1983).
24. Newton, R. *et al.* Plasma and salivary pharmacokinetics of caffeine in man. *Eur. J. Clin. Pharmacol.* **21**, 45–52 (1981).
25. Tarnopolsky, M. A. Caffeine and creatine use in sport. *Ann. Nutr. Metab.* **57 Suppl 2**, 1–8 (2010).
26. Alharbi, O., Xu, Y. & Goodacre, R. Simultaneous multiplexed quantification of caffeine and its major metabolites theobromine and paraxanthine using surface-enhanced Raman scattering. *Anal. Bioanal. Chem.* **407**, 8253–61 (2015).
27. Arnaud, M. J. Pharmacokinetics and metabolism of natural methylxanthines in animal and man. *Handb. Exp. Pharmacol.* **200**, 33–91 (2011).
28. Bishop, D. Dietary supplements and team-sport performance. *Sports Med.* **40**, 995–1017

(2010).

29. Jiang, X., Zhang, D. & Jiang, W. Coffee and caffeine intake and incidence of type 2 diabetes mellitus: a meta-analysis of prospective studies. *Eur. J. Nutr.* **53**, 25–38 (2014).
30. de Mejia, E. G. & Ramirez-Mares, M. V. Impact of caffeine and coffee on our health. *Trends in Endocrinology and Metabolism* (2014). doi:10.1016/j.tem.2014.07.003
31. Association, A. P. *Diagnostic and statistical manual of mental disorders (4th ed.). Alzheimer Disease Associated Disorders* (1994). doi:10.1097/00002093-198802020-00022
32. Jain, S., Srivastava, A. S., Verma, R. P. & Maggu, G. Caffeine addiction: Need for awareness and research and regulatory measures. *Asian Journal of Psychiatry* (2017). doi:10.1016/j.ajp.2017.01.008
33. Beauchamp, G., Amaducci, A. & Cook, M. Caffeine Toxicity: A Brief Review and Update. *Clin. Pediatr. Emerg. Med.* **18**, 197–202 (2017).
34. Holmgren, P., Nordén-Pettersson, L. & Ahlner, J. Caffeine fatalities--four case reports. *Forensic Sci. Int.* **139**, 71–3 (2004).
35. PETERS, J. M. Factors Affecting Caffeine Toxicity: A Review of the Literature. *J. Clin. Pharmacol. J. New Drugs* **7**, 131–141 (1967).
36. Rodopoulos, N., Wisén, O. & Norman, A. Caffeine metabolism in patients with chronic liver disease. *Scand. J. Clin. Lab. Invest.* **55**, 229–42 (1995).
37. Conte, E. D., Barry, E. F. & Rubinstein, H. Determination of Caffeine in Beverages by Capillary Zone Electrophoresis: An Experiment for the Undergraduate Analytical Laboratory. *J. Chem. Educ.* **73**, 1169 (1996).
38. Flavin, K. & Resmini, M. Molecular Imprinting with Nanomaterials. in *Advanced Nanomaterials* **2**, 651–675 (Wiley-VCH, 2010).
39. Chen, L., Wang, X., Lu, W., Wu, X. & Li, J. Molecular imprinting: perspectives and applications. *Chem. Soc. Rev.* (2016). doi:10.1039/C6CS00061D
40. Ahmad Bhawani, S., Fong, S. S. & Mohamad Ibrahim, M. N. Spectrophotometric Analysis of Caffeine. *Int. J. Anal. Chem.* **2015**, 1–7 (2015).
41. Antuña-Jiménez, D. *et al.* Chapter 1 - Molecularly Imprinted Electrochemical Sensors: Past, Present, and Future. in *Molecularly Imprinted Sensors* (2012). doi:http://dx.doi.org/10.1016/B978-0-444-56331-6.00001-3

42. Analysis of coffee bean extracts by use of ultra-performance liquid chromatography coupled to quadrupole time-of-flight mass spectrometry. *MethodsX* **1**, 264–268 (2014).

43. Svítková, J., Machková, M., Šatkovská, P., Cinková, K. & Švorc, Ľ. Utilization of electrochemical methods in determination of trace elements in beverages. doi:10.2478/v10188-012-0007-1

44. Sharma, P. S., Pietrzyk-Le, A., D'Souza, F. & Kutner, W. Electrochemically synthesized polymers in molecular imprinting for chemical sensing. *Anal. Bioanal. Chem.* **402**, 3177–3204 (2012).

45. Kan, X. *et al.* A novel electrochemical sensor based on molecularly imprinted polymers for caffeine recognition and detection. *J. Solid State Electrochem.* **16**, 3207–3213 (2012).

46. Pauling, L. A Theory of the Structure and Process of Formation of Antibodies [*]. *J. Am. Chem. Soc.* **62**, 2643–2657 (1940).

47. PAULING, L. & CAMPBELL, D. H. THE PRODUCTION OF ANTIBODIES IN VITRO. *Science (80-.).* **95**, 440–441 (1942).

48. Alizadeh, T. Comparison of different methodologies for integration of molecularly imprinted polymer and electrochemical transducer in order to develop a paraoxon voltammetric sensor. *Thin Solid Films* **518**, 6099–6106 (2010).

49. Figueiredo, E. C. *et al. Impressão molecular: uma estratégia promissora na elaboração de matrizes para a liberação controlada de fármacos*. *Revista Brasileira de Ciências Farmacêuticas Brazilian Journal of Pharmaceutical Sciences* **44**, (2008).

50. Tarley, C. R. T., Sotomayor, M. D. P. T. & Kubota, L. T. Polímeros biomiméticos em química analítica. Parte 2: aplicações de MIP ("Molecularly Imprinted Polymers") no desenvolvimento de sensores químicos. *Quim. Nova* **28**, 1087–1101 (2005).

51. Yilmaz, E., Mosbach, K. & Haupt, K. Influence of functional and cross-linking monomers and the amount of template on the performance of molecularly imprinted polymers in binding assays. *Anal. Commun.* **36**, 167–170 (1999).

52. Foguel, M. V. *et al.* Synthesis and evaluation of a molecularly imprinted polymer for selective adsorption and quantification of Acid Green 16 textile dye in water samples. *Talanta* **170**, 244–251 (2017).

53. EL-Sharif, H. F., Yapati, H., Kalluru, S. & Reddy, S. M. Highly selective BSA imprinted

polyacrylamide hydrogels facilitated by a metal-coding MIP approach. *Acta Biomater*. **28**, 121–127 (2015).

54. Pauling, L. *et al.* Molecularly Imprinted Polymers for Solid Phase Extraction. *Sensors Actuators B Chem.* **173**, 591–598 (2012).
55. Sociedade Brasileira de Química. *Química nova : publication of the Sociedade Brasileira de Química*. (SBQ).
56. Appell, M., Kendra, D. F., Kim, E. K. & Maragos, C. M. Synthesis and evaluation of molecularly imprinted polymers as sorbents of moniliformin. *Food Addit. Contam.* **24**, 43–52 (2007).
57. Iturralde, I., Paulis, M. & Leiza, J. R. The effect of the crosslinking agent on the performance of propranolol imprinted polymers. *Eur. Polym. J.* **53**, 282–291 (2014).
58. Vasapollo, G. *et al.* Molecularly imprinted polymers: Present and future prospective. *Int. J. Mol. Sci.* **12**, 5908–5945 (2011).
59. Chen, L., Wang, X., Lu, W., Wu, X. & Li, J. Molecular imprinting: perspectives and applications. *Chem. Soc. Rev.* **45**, 2137–2211 (2016).
60. Wong, A. *et al.* DEVELOPMENT OF AN ELECTROCHEMICAL SENSOR MODIFIED WITH MWCNT-COOH AND MIP FOR DETECTION OF DIURON. *Electrochim. Acta* **182**, 122–130 (2015).
61. Yilmaz, E., Mosbach, K. & Haupt, K. Influence of functional and cross-linking monomers and the amount of template on the performance of molecularly imprinted polymers in binding assays. *Anal. Commun.* (1999). doi:10.1039/a901339c
62. Sellergren, B. *Molecularly imprinted polymers : man-made mimics of antibodies and their applications in analytical chemistry*. (Elsevier, 2001).
63. Sergey, P. & Anthony, T. *Molecular Imprinting of Polymers*. *Technology* (2006).
64. Zhu, H. *et al.* Synthesis of a core–shell magnetic Fe_3O_4–NH_2@PmPD nanocomposite for efficient removal of Cr(vi) from aqueous media. *RSC Adv.* **7**, 36231–36241 (2017).
65. Lv, Y., Tan, T. & Svec, F. Molecular imprinting of proteins in polymers attached to the surface of nanomaterials for selective recognition of biomacromolecules. *Biotechnology Advances* **31**, 1172–1186 (2013).
66. Ton, X. A. *et al.* A versatile fiber-optic fluorescence sensor based on molecularly imprinted microstructures polymerized in situ. *Angew. Chemie - Int. Ed.* **52**, 8317–8321

(2013).

67. Zoppe, J. O. *et al.* Surface-Initiated Controlled Radical Polymerization: State-of-the-Art, Opportunities, and Challenges in Surface and Interface Engineering with Polymer Brushes. *Chem. Rev.* **117**, 1105–1318 (2017).

68. Reyes-Gallardo, E. M., Lucena, R., Cárdenas, S. & Valcárcel, M. Polymer–nanoparticles composites in bioanalytical sample preparation. *Bioanalysis* **7**, 1723–1730 (2015).

69. Pan, J. *et al.* Magnetic molecularly imprinted microcapsules derived from Pickering emulsion polymerization and their novel adsorption characteristics for λ-cyhalothrin. *RSC Adv.* **4**, 4435–4443 (2014).

70. Gupta, A. K. & Gupta, M. Synthesis and surface engineering of iron oxide nanoparticles for biomedical applications. *Biomaterials* **26**, 3995–4021 (2005).

71. Kafrouni, L. & Savadogo, O. Recent progress on magnetic nanoparticles for magnetic hyperthermia. *Prog. Biomater.* **5**, 147–160 (2016).

72. Zhu, M., Wang, Y., Meng, D., Qin, X. & Diao, G. Hydrothermal Synthesis of Hematite Nanoparticles and Their Electrochemical Properties. *J. Phys. Chem. C* **116**, 16276–16285 (2012).

73. Ramimoghadam, D., Bagheri, S., Bee, S. & Hamid, A. Progress in electrochemical synthesis of magnetic iron oxide nanoparticles. *J. Magn. Magn. Mater.* **368**, 207–229 (2014).

74. Ashjari, M., Mahdavian, A. R., Ebrahimi, N. G. & Mosleh, Y. Efficient Dispersion of Magnetite Nanoparticles in the Polyurethane Matrix Through Solution Mixing and Investigation of the Nanocomposite Properties. *J. Inorg. Organomet. Polym. Mater.* **20**, 213–219 (2010).

75. Wang, X., Wang, L., He, X., Zhang, Y. & Chen, L. A molecularly imprinted polymer-coated nanocomposite of magnetic nanoparticles for estrone recognition. *Talanta* **78**, 327–332 (2009).

76. Kong, X., Gao, R., He, X., Chen, L. & Zhang, Y. Synthesis and characterization of the core-shell magnetic molecularly imprinted polymers (Fe_3O_4@MIPs) adsorbents for effective extraction and determination of sulfonamides in the poultry feed. *J. Chromatogr. A* **1245**, 8–16 (2012).

77. Gimbert, F., Morin-Crini, N., Renault, F., Badot, P.-M. & Crini, G. Adsorption isotherm

models for dye removal by cationized starch-based material in a single component system: Error analysis. *J. Hazard. Mater.* **157**, 34–46 (2008).

78. Allen, S. J., Mckay, G. & Porter, J. F. Adsorption isotherm models for basic dye adsorption by peat in single and binary component systems. *J. Colloid Interface Sci.* **280**, 322–333 (2004).
79. Ali, M. M., Eisa, M., Taha, M. I., Zakaria, B. A. & Elbashir, A. A. Determination of caffeine in some Sudanese beverages by High Performance Liquid Chromatography. *Pakistan J. Nutr.* **11**, 336–342 (2012).
80. Ben Aissa, A., Herrera-Chacon, A., Pupin, R. R., Sotomayor, M. D. P. T. & Pividori, M. I. Magnetic molecularly imprinted polymer for the isolation and detection of biotin and biotinylated biomolecules. *Biosens. Bioelectron.* **88**, 101–108 (2017).
81. Pan, J. *et al.* Magnetic molecularly imprinted polymers based on attapulgite/Fe3O4 particles for the selective recognition of 2,4-dichlorophenol. *Chem. Eng. J.* **174**, 68–75 (2011).
82. Zougagh, M., Ríos, A. & Valcárcel, M. Automatic selective determination of caffeine in coffee and tea samples by using a supported liquid membrane-modified piezoelectric flow sensor with molecularly imprinted polymer. *Anal. Chim. Acta* (2005). doi:10.1016/j.aca.2005.02.060
83. Sodipo, B. K. & Aziz, A. A. Recent advances in synthesis and surface modification of superparamagnetic iron oxide nanoparticles with silica. *J. Magn. Magn. Mater*. **416**, 275–291 (2016).
84. Marestoni, L. D. [UNESP]. Simula{ç}{ã}o computacional e s{í}ntese de polímero molecularmente impresso para extra{ç}{ã}o em fase s{ó}lida (MISPE) de ciprofloxacina em urina. *Aleph* 167 f. : il. (2014).